



Originally published as:

Tolksdorf, J. F., Schröder, F., Petr, L., Herbig, C., Kaiser, K., Kocar, P., Fulling, A., Heinrich, S., Hönig, H., Hemker, C. (2020): Evidence for Bronze Age and Medieval tin placer mining in the Erzgebirge mountains, Saxony (Germany). - *Geoarchaeology*, 35, 2, 198-216.

<https://doi.org/10.1002/gea.21763>

## **Evidence for Bronze Age and Medieval tin placer mining in the Erzgebirge mountains, Saxony (Germany)**

Johann Friedrich Tolksdorf<sup>1\*</sup> [orcid.org/0000-0002-8180-6115], Frank Schröder<sup>1</sup>, Libor Petr<sup>2</sup>, Christoph Herbig<sup>3</sup>, Knut Kaiser<sup>4</sup> [orcid.org/0000-0002-5080-6075], Petr Kočár<sup>5</sup>, Alexander Füllung<sup>6</sup>, Susann Heinrich<sup>7</sup>, Heide Höning<sup>1</sup>, Christiane Hemker<sup>1</sup>

<sup>1</sup>Archaeological Heritage Office of Saxony, ArchaeoMontan Research Group, Dresden

<sup>2</sup>Department of Botany and Zoology, Faculty of Science, Masaryk University Brno

<sup>3</sup>University of Frankfurt/Main, Institute for Archaeological Sciences

<sup>4</sup>Helmholtz Centre Potsdam, German Research Centre for Geosciences GFZ, Potsdam

<sup>5</sup>Czech Academy of Sciences, Institute of Archaeology, Praha

<sup>6</sup>Humboldt University of Berlin, Luminescence Laboratory

<sup>7</sup>Max Planck Institute for Evolutionary Anthropology, Department of Human Evolution, Leipzig

### *Keywords*

Bronze Age economy, tin mining, palaeoenvironmental reconstruction, alluvial sedimentation, OSL, anthracology, micromorphology

### *Abstract*

Tin is an essential raw material both for the copper-tin alloys developed during the Early Bronze Age and for the casting of tableware in the Medieval period. Secondary geological deposits in the form of placers (cassiterite) provide easily accessible sources but have often been reworked several times during land-use history. In fact, evidence for the earliest phase of tin mining during the Bronze Age has not yet been confirmed for any area in Europe, stimulating ongoing debate on this issue. For this study a broad range of methods (sedimentology, pedology, palynology, anthracology, OSL/<sup>14</sup>C-dating, micromorphology) was applied both within the extraction zone of placer mining and the downstream alluvial sediments at Schellerhau site in the upper eastern Erzgebirge (Germany). The results indicate that the earliest local removal of topsoil and processing of cassiterite-bearing weathered granite occurred already in the early second millennium BC, thus coinciding with the early and middle Bronze Age period. Placer mining resumed in this area during the Medieval period, probably as early as the 13th century AD. A peak of alluvial sedimentation during the Mid-15th century AD is probably related to the acquisition of this region by the Elector of Saxony and the subsequent promotion of mining.

### *Introduction*

Tin is an essential raw material for the production of tin-copper alloys that first became common during the Early Bronze Age. As the occurrence of tin bearing mineral deposits is confined to only very few areas in Eurasia, mainly Iberia, Cornwall, Normandy and the Erzgebirge (Ore Mountains/ Krušné hory) as well as the Middle East, the location of mining

sites and the distribution, exchange and circulation patterns of tin have been the focus of archaeological research for decades (Penhallurick, 1986; Muhly, 1985; Roden, 1985; Rahmstorf, 2016). In spite of intensive research, neither the rich placer deposits of Cornwall (Thorndycraft, Pirrie, & Brown, 2004; Meharg et al., 2012) nor investigations in the Erzgebirge (Bouzek, Koutecký, & Simon, 1989; Bartelheim & Niederschlag, 1998; Bartelheim, Niederschlag, & Rehren, 1998) have produced any unquestionable archaeological evidence of Bronze Age mining activities so far. Moreover, recent attempts to trace the origin of tin used for Bronze Age alloys by means of lead (Niederschlag et al., 2003) and tin isotopes (Haustein, Gillis, & Pernicka, 2010; Brüggmann et al., 2015; Nessel, Brüggmann, & Pernicka, 2015; Marahrens et al., 2015; Brüggmann et al., 2017) indicate considerable overlaps in the geochemistry of European tin deposits. While it is widely assumed that the extraction of tin in the form of cassiterite placers (SnO<sub>2</sub>) from secondary fluvial deposits is the most efficient and economic technique and has most likely been performed during the Bronze Age period, the environmental setting makes archaeological identification generally difficult. In addition to the assumed scarcity of artefacts and building structures related to placer mining, the impact of extensive mining activities and the associated destruction/alteration of earlier mining relicts during medieval and modern times poses strong obstacles to any unambiguous identification of older activities (Hemker & Elburg, 2013) as they create an archaeological ‘palimpsest’.

The key element of placer mining is the processing of weathered bedrock and fluvial deposits in large quantities using streaming water. While lighter materials and fine sediments are carried away by the water in ditches or natural courses and are often deposited downstream, larger material like gravels and the target material with higher density (tin) are retained in mobile troughs or sluice boxes that follow the advancing face of sediment excavation. While the target material is collected for further processing, the gravels need to be cleared regularly from the troughs and boxes and are usually stacked in the immediate vicinity (Agricola, 1556; Nelson & Church, 2012). After the end of the often seasonal mining operations, the sluice boxes and troughs are often either dismantled or discarded leaving behind areas to the sides of the valley floor that resemble huge open-cast mining with characteristic stacked overburden gravels and ditches but only very few artefacts (picks, ceramics, sluice box remains). Given the expected scarcity of archaeological features and in respect of resuming mining activities in later periods, geoarchaeological approaches (sedimentology, pedology, anthracology, palynology, anthracology, and micromorphology) provide the only chance to resolve this problem and to reconstruct mining phases in a higher chronological and spatial resolution. Especially promising are the former surfaces of the sediment extraction preserved below the

stacked gravel heaps as well as the zone of potential sedimentation in the ditches and downstream.

### ***Relicts of placer mining at Schellerhau***

The study site is situated in the eastern part of the Erzgebirge Mountains near Altenberg (50.76°N / 13.72°E) at an altitude of about 740 m asl (Fig. 1A, B). Here the spring of the Rote Weißeritz river cuts through the Schellerhau granite formation that contains tin in the form of greisen mineralization (Müller, Seltmann, & Behr, 2000; Fedkin, Seltmann, & Förster, 2001) (Fig. 1C). A digital elevation model with a spatial resolution of 20x20 cm reveals extensive excavations in the Schellerhau granite with heaps, ditches and hollows (Fig. 2 and 3A). The first historical records of tin trade from the wider Erzgebirge area are very unspecific and comprise, for example, the drop of prices for tin from Cornwall on the market of Cologne due to first imports from Germany in AD 1241, and the first pewter objects having appeared in central Germany around AD 1250 (Berger, 2014). The first historical record of tin mining which relates directly to an area in the Erzgebirge dates to AD 1305, referring to tin mining activities at Crupa (= Graupen / Krupka), approx. 15 km SE of Schellerhau (Emler, 1882, No. 2041). The first mention of placer mining (German: Seifen) in the vicinity of the site is provided by a record from AD 1464. A number of legal documents covering the time period AD 1573-1735 can be related to placer mining activities and to an ore stamp mill in the investigated area, while the village of Schellerhau was founded in AD 1543 to supply Altenberg with rural products and charcoal (Hammermüller, 1964). The area surrounding the spring of the Rote Weißeritz river was heavily altered by the ditch system of the Neugraben stream collecting water for the Großer Galgenteich basin, built in AD 1550-1553 to power hammer mills and the construction of the Speicher Altenberg basin, built in AD 1992 to provide drinking water.

### ***Methods and material***

Based on modern analogies, the spatial structure of placer mining sites can be subdivided into an extraction zone and a corresponding downstream sedimentation zone (Fig. 2). Within the extraction zone, fluvial deposits and highly weathered bedrock were washed to separate the heavy ore placers from the lighter geological components. Characteristic features are ditches to supply water for this process, technical infrastructures like sluice boxes and heaps of coarse matter (gravels to boulders) sorted out during washing. In the process of sluicing, fine-grained



material is transported downstream and triggers increased overbank deposition along the river (Knighton, 1987; L. A. James, 1991; A. James, 1999; Hilmes & Wohl, 1995; Nelson & Church, 2012).

Construction of the chronology of the site is based on 17  $^{14}\text{C}$  samples, 4 OSL-samples. All  $^{14}\text{C}$  analyses were performed by the CEZ Mannheim and calibrated according to the IntCal13 dataset (Reimer, 2013) (Tab.1). Optically stimulated luminescence (OSL) was used to estimate the time of the last exposure of quartz grains to sunlight (=deposition/burial of sediments) and performed at the Luminescence laboratory of HU Berlin university using a Risø TL/OSL-DA 15C/D unit (Tab.2). Measurement of the equivalent dose (DE) was performed on quartz particles of 90-200 $\mu\text{m}$  in size after standard treatment with HCl (10%) and H<sub>2</sub>O<sub>2</sub> (10%) to remove carbonates and organic material. After removal of feldspars, etching with HF (40%), and mounting of aliquots using a 1mm/2 mm stencil, preheat- and dose recovery tests were performed to ensure optimal measurement by SAR protocol (Murray & Wintle, 2000; Wintle & Murray, 2006). While DE distribution of sample HUB-0751 indicated well bleached material and allowed for the application of a Central Age Model (CAM), skewed distributions in samples HUB-0752 and HUB-754 indicated poor bleaching that did not completely delete signals from older relocation events. Consequently, a Minimum Age Model (Galbraith et al., 1999) was applied calculating the overdispersion with  $\square b=0,1$  and  $\square b=0,2$ . Based on the extremely skewed distribution in HUB-0754 an additional age estimate was calculated using the lowest aliquot measurement only. As measurements from HUB-0753 provided extremely high DE values, far beyond the scope of this study, calculation was based on the mean values. Dose rate calculation was performed using DRAC software (Durcan, King, & Duller, 2015) based on  $^{238}\text{U}$ / $^{232}\text{Th}$ / $^{40}\text{K}$  concentration measured by gamma-ray spectroscopy in the sediment, the water content and the cosmic dose based on the parameters sediment depth, geographical position/elevation. A disequilibrium was detected in the  $^{238}\text{U}$  series of HUB-0753, probably due to secondary  $^{238}\text{U}$  enrichment in the sediment, and therefore the minimum / maximum  $^{238}\text{U}$  content was calculated based on different isotopic series.

Palynological samples (n=22) were prepared according to the acetolysis method (Moore, Webb, & Collinson, 1991; Berglund & Ralska-Jasiewiczowa, 1986). A minimum of 500 palynomorphs was identified for each sample based on the standard literature (Beug, 2004). During the counting, the amount of charcoal particles was recorded without size classification (Clark, 1984).

Botanical macro-remains were retrieved from sediment samples by a combined flotation and wet sieving procedure (2, 1, 0.5, 0.25 mm mesh width). While the anthracological identification of charcoal particles followed wood-anatomical criteria (Schweingruber, 1990), the identification of charred and subfossil botanical remains was based both on literature (Cappers, Bekker, & Jans, 2012) and the reference collection at the University of Frankfurt. The attribution of the identified taxa to plant communities and specific habitats is based on Oberdorfer (2001) (Tab. 3).

A thin section for micromorphological analysis was prepared from a sediment monolith in profile 9 impregnated with resin. The thin section was examined at the Max-Planck-Institute for Evolutionary Anthropology with a petrographic microscope under plane- and crossed polarised light. Microscopic description (SI 1) followed the nomenclature of Bullock (1985) and Stoops (2003).

After a field survey in 2016, eleven soil profiles were dug both in the extraction zone and in the sedimentation zone of Schellerhau (SI 2). Soil horizons were recorded and sampled according to the guidelines of the German soil classification (AG Boden, 2005) and an international standard (FAO, 2006). A total of 28 samples were subjected to sedimentological laboratory analyses on the matrix matter <2 mm in order to assist the designation of sedimentary facies and diagnostic soil horizons (SI 2). For grain size analysis, samples were air dried and hand-crushed. If present, organic matter was removed using 30% H<sub>2</sub>O<sub>2</sub>. Grain-size distribution was determined by a laser diffraction test (Beckman-Coulter particle analyzer LS 13320). The content of organic matter was estimated by combustion at 550 °C (loss-on-ignition, LOI).

## ***Results***

### **Stratigraphy in the zone of downstream sedimentation**

The onset of alluvial sedimentation in all four profiles along the Rote Weißeritz river is characterised by silty material with abundant charred material (Fig. 2). Profile 11 is situated immediately downstream the largest extraction zone and charred material from the basal alluvial sediments here yielded 14C ages of 1280-1391 calAD (MAMS-33865, charred short lived material) and 1027-1154 calAD (MAMS-31409, charcoal), respectively. OSL analysis from this layer revealed a wide range of equivalent doses between the aliquots, typical for incomplete bleaching of older material. Consequently, the minimum age of deposition has been calculated to  $1.0 \pm 0.07$  ka (HUB-0754). The botanical spectrum (sample B5) from this

layer comprises *Rubus idaeus* (raspberry), *Sambucus nigra* (elder), *Picea abies* (spruce) and *Juncus* (rush).

Profile 4 is situated a little further downstream (Fig. 2& 3F). A layer of charcoals particles from the lowermost layer of silt yielded a 14C age of 1436-1497 / 1600-1615 calAD (MAMS-28840). OSL analysis of this sediment unit yielded an age of  $0.9 \pm 0.03$  ka (HUB-0751), thereby supporting the 14C calibration interval within the 15th century AD. The charcoal spectrum from this basal unit (sample C3) only contained *Picea abies*. An upper layer of silty material in this profile provided a minimum OSL age of  $0,93 \pm 0,12$  ka (HUB-0752). The charcoal concentration in the uppermost part of the profile (sample C1) consisted mainly of *Picea abies* with some *Abies alba* (fir).

Profile 12, situated at the outlet of an artificial channel cutting a river meander, featured three sediment units resulting from deposition of fine material (Fig. 2 & 3D). Within the uppermost layer of fine sand, a layer of *Picea abies* needles (sample B8) and high organic content occurs. Beside long hand-forged iron nails, it contained numerous pieces of charcoal of *Picea abies* (sample C4) that were 14C-dated to the 17th century AD or later. While the silty sediment unit in the middle of the profile contained small charcoal particles with 14C-ages from 1437-1498/1508-1510/1600-1616 calAD (MAMS-31791), the basal fine sediment unit yielded a 14C-age of 1424-1460 calAD (MAMS-32964).

The onset of fine overbank sedimentation overlying the gravel bed is also evident further downstream in profile 10, where charred particles are 14C dated to 1440-1511 /1600-1616 calAD (MAMS-32963).

### **Stratigraphy in the extraction zone**

To study the structure of the extraction zone, seven profiles in the form of a W-E transect covering different topographic elements of the placer mining zone were examined (Fig. 4). As a reference, profile 8 recorded stratigraphic conditions immediately outside the open cast area. The granite here was strongly weathered with grain size classes in the silt and sand fraction. It was covered by periglacial loess, subsequent coarse solifluction debris (cover bed) and finally peat (Fig. 3B). A sequence of eight pollen spectra covering the peat layer in the uppermost 30 cm of the profile proves its development during the whole Holocene. Based on the dominance of *Pinus* with the absence of taxa like *Fagus* and *Abies* and very low percentages of *Picea*, the lowermost sample at 30cm depth can be ascribed to the Preboreal period (Fig. 6A). The samples at 25 and 20 cm depth show high values of *Corylus avellana* and the replacement of *Pinus* by *Picea*, *Tilia*, *Quercus* and later *Fagus*. While *Abies* and *Carpinus betulus* are still

absent at 15 cm depth, both taxa are well-established at 13 cm depth. Although the first Cerealia-type pollen appear at 11 cm depth, the continuous absence of other settlement related taxa like *Plantago lanceolata*, *Centaurea cyanus* or *Rumex acetosella* indicate that they probably derive from long-distance transport and do not mirror settlement activity in the nearby vicinity. Charcoal particles are present at all depths.

Profile 9 is situated at the bottom of the open-cast mining area that is more than 3.5 m below the surrounding area. At a depth of 50/55 cm below surface, weathered granite forms an undulating surface that is covered by a dark layer rich in organic material and charcoals (Fig. 5A, layer B). Immediately above this organic layer are 40 cm of gravels without any fine material, representing stacked oversize pieces of gravel from the placer mining process (Fig. 5A, layer C). Micromorphological analysis of the organic layer (Fig. 5C, SI 1) and the contact zone to the weathered granite show three units: The lowermost material (unit 3) can be characterised as in situ weathered bedrock material. Several cracks, sporadically used as root channels and weakly weathered mineral grains were identified. The unit shows a rough surface with partly detached mineral grains. The overlying material (unit 2) is loosely packed and rich in organic matter as a result of strong bioturbation. Numerous roots, root residues, faecal pellets, sclerotia, residues of mycorrhiza mantles and the partly crumb microstructure underline the efficacy of biogenic processes forming a palaeo-surface. The high abundance of microcharcoal and larger charcoal fragments (up to 4 mm in diameter) augment the dark colouring of the material that is mainly caused by the high amount of organic material such as plant residues and amorphous organic fine material partly masking the mineral grains (coatings). The uppermost unit (unit 1) consists of mineral material (granite rock fragments and mineral fine material) and organic material (roots, plant residues, amorphous organic fine material). The lighter colour in comparison to the underlying material is a result of less abundant charcoal fragments and lower contents of organic matter. The material is only moderately affected by bioturbation and therefore more densely packed.

Botanical analyses on subsamples from the organic layer (samples B1-B4) contained large quantities of *Picea abies* needles with a high share of charred needles in the lower part, the contact zone to the weathered granite and decreasing percentages of charred material towards the upper part (Fig. 6B). High numbers of uncharred remains of *Juncus spec.* were found in these samples as well as sporadic evidence for *Oxalis acetosella* or *Rubus idaeus*. Additionally, a sample of 50 larger (> 0.6 mm size) charcoal particles, was found to include wood of *Picea abies* exclusively (sample C2), yielding 14C- ages of 2012-1858 calBC (MAMS-30188) and 2016-1780 cal BC (MAMS-31792). OSL dating of this layer provided

an age of  $77.83 \pm 5.12$  ka (HUB-0753), indicating incomplete bleaching of the sample, i.e. no exposition to sunlight. The pollen spectrum of this layer is characterised by very low percentages of *Abies* pollen. *Carpinus betulus* or Cerealia-type pollen are still absent. Thus a biostratigraphical position comparable to the depth between 15 and 13 cm in profile 8 with no signs of later alteration, i.e. during the late Holocene, becomes apparent (Figs. 6A&B). However, the concentration of charcoal particles is much higher than in any sample from profile 8.

Profile 6 enabled the sampling of a 75 cm sequence of peat with intercalating layers of fluvial sand that postdate the use of a ditch in the placer mining area (Fig. 3E). A 14C age from the lowermost part of the peat yielded an age younger than the Mid-17th century AD (1680-1938 calAD, MAMS-30240). This is corroborated by a sequence of 10 pollen samples that presents a typical (very) late-Holocene vegetation composition. Remarkable is the only sporadic and rather late appearance of Cerealia-type pollen at a depth of 54 cm. Compared to profiles 8 and 9, samples from this ditch stand out by boasting a high share of Poaceae pollen reflecting typical vegetation elements in open wetland patches. After abandonment of the ditch it aggraded rather fast by peat accumulation alternating with deposition of fluvial sands during high-energy flooding events.

Profiles 5 and 7 prove the large extent of the piled up gravel material in the form of ridges of different height on the floor of the extraction zone (Fig. 3C). In profile 5, charcoal particles from a humic horizon situated below one meter of gravel yielded ages of 1433-1371/1359-1300 calBC (MAMS-31407) and 1499-1393/1333-1327 calBC (MAMS-33873). A shallow depression to the east of these mining heaps was sampled in profile 13. Here, mining heap material is covered by an 80 cm thick sequence of organic detritus (gyttja) with layers of organic silt and sand in the uppermost part. A botanical sample from the organic detritus yielded only a few *Picea* needles (47 uncharred /1 charred), while an abundance of *Picea* needles in the covering silt (>10,000) together with seeds of *Juncus* spec., fruits of *Carex* spec., and the sediment type indicate that sedimentation must have occurred in a wet environment with low transport energy. 14C analyses on two of the few pieces of charcoal yielded ages of 3084-2911 calBC (75 cm depth, MAMS-32528) and 5206-4933 calBC (62cm depth, MAMS-32529) respectively. The inversion of the dates in relation to their stratigraphic position indicates that the charcoal particles represent relocated older material, probably from the peat layer originally covering the undisturbed site, as is the case in profile 8. 14C analyses on a charcoal embedded in the upper part of the basal mining heap yielded an age of 8739-

8549 calBC (MAMS-34615) and the subfossil *Picea* needles in the silt provided a maximum age of 1651 calAD (MAMS-33868).

A potential source for the input of older charcoal material was identified by means of profile 3, situated on the top of a central ridge within the mining area, where a layer of fluvial sand is covered by 15 cm of peat and containing charcoal fragments of Mid-Holocene age (6205-6009 calBC; MAMS-28839). This peat layer can therefore be linked to the palynostratigraphically dated peat of profile 8. It shows the (fluvio-) stratigraphical setting prior to human activity and the existence of a former river branch, representing the starting point for the placer mining.

## ***Discussion***

### **Site formation and mining history at Schellerhau**

The palynological results from profile 8, as well as the dated charcoals from profile 3 and 13, show the abundance of charcoal of Early to Mid-Holocene age in the peat layer that must have covered the whole area (Fig. 4B). This is in good accordance with other palynological stratigraphies in the upper Erzgebirge region, where charcoals fragments dating to these periods are found regularly (Stebich, 1995; Seifert-Eulen, 2016). During the removal of the peat in the course of the mining activities, the pieces of charcoals were remobilised as indicated by the stratigraphically inverted 14C ages in the silted up depression at profile 13 (Figs. 7&8). The distinct layers of sandy material recorded in profile 6 and 13 indicate that such relocation probably occurred during episodic flash flood events.

However, a similar process is unlikely for the charcoals analysed from the layers below the mining heaps in profiles 9 and profile 5. Micromorphological results from profile 9 show that the underlying material (unit 3) consists almost completely of slightly weathered bedrock (granite), whereas the overlying material (units 1 and 2) contains more strongly weathered fine mineral material, organic matter and high amounts of (micro-) charcoal. The absence of a transitional zone with moderately to highly weathered granite or a cover-bed (Lehmann & Präger, 1992; Kleber et al., 2013) and the sharp boundary between the highly contrasting substrates suggest a deposition of dislocated soil material on a bare bedrock surface rather than in situ soil formation. This dislocated material was further altered by bioturbation after deposition. A pure biogenic formation of the material can be excluded as the most abundant voids are packing voids and the traces of bioturbational activity are only moderately developed (especially in unit 1). A connection of this layer with human activities involving

burning is further underlined by the concentration of charred *Picea* needles in the lower part of units 1 and 2, which must have developed after the complete removal of the topsoil and the zone of highly weathered bedrock. Together with the subsequent piled up coarse gravels on top of this discordance, the deep removal of soil and the formation of this layer can be explained as part of local placer mining activities that targeted the highly weathered upper layers of the greisen formation. Based on the <sup>14</sup>C ages from profiles 5 and 9, this removal of highly weathered bedrock material and formation of the organic layer must have occurred during the 20th-19th century BC and the 15th/14th century BC, respectively (Figs. 7 & 8). A later formation of the organic layer in profile 9 with an incorporation of older charcoal particles is precluded by the biostratigraphically characteristic very low values of *Abies* pollen and the complete absence of *Carpinus betulus* and *Cerealia*-type pollen that should be expected to be much higher if the layer was open to pollen influx later than the Subboreal period. The onset of medieval placer mining in this area is indicated by the onset of silty sedimentation in profile 11 that contains taxa typically associated with clearances like *Rubus idaeus* or *Sambucus nigra* dating to the 13th/14th century (Fig. 7). It is in accordance with the first historical evidence of tin placer mining in the Erzgebirge from the early 14th century AD (Wagenbreth, 1990). The 15th century AD stands out as a phase of extreme overbank deposition visible in profiles 12, 4 and 10. It corresponds with the first historical sources mentioning the onset of the underground mining of tin greisen in the nearby Altenberg in 1436/1440 AD and the acquisition of the mining district by Elector Friedrich II. of Saxony in 1446 AD. These pieces of evidence may therefore mark the intensified development of mining (Wagenbreth, 1990, pp. 159–164). Most of the ditches in the mining area are chronologically related to this time period. They were either used for washing of coarse material or for diverting water to sluice boxes. After their abandonment they were filled with peat and sand as well as relocated charcoal fragments (Fig. 8).

No deposition related to the Bronze Age was recorded in the profiles downstream. This can be explained either by the smaller amount of material that was released into the stream at the time or by subsequent fluvial erosion. Relocation of older fluvial sediments during the Medieval period is indicated by the DE-distribution visible in OSL-measurements HUB-0752 and HUB-0754, showing the presence of poorly bleached older sediments resulting in a minimum-age estimate. A generally strong coupling between the amount of fine material released by placer mining activities and the formation of overbank deposition downstream is supported by the comparatively thin sandy fluvial layers that are associated with the Modern period (profiles 10 and 12; Fig 8).

### **Bronze Age tin placer mining at Schellerhau**

While there is no archaeological evidence for permanent prehistoric settlement in the Erzgebirge area, a small assemblage of prehistoric ceramics near the tin placer deposits of the Sauschwemme site (Fig. 1B) in the western part of the Erzgebirge and a limited number of stray finds have been discussed to reflect temporary human presence for mining purposes at higher altitudes (Bouzek, Koutecký, & Simon, 1989; Bartelheim, Niederschlag, & Rehren, 1998; Bartelheim & Niederschlag, 1998). Although no traces of constructions or processing remnants have been observed at Schellerhau, the deep digging into the weathered granite bedrock and the superimposed layer of piled up gravels indicate the extraction of tin by some kind of washing/sluicing process. Effective constructions related to the separation of ore minerals were in use during the Bronze Age, which is evident from the Troiboden site in Austria, where a wooden box was used to enrich copper ores by flotation between compartments, dendrochronologically dated to 1375 BC (Stöllner et al., 2010).

The interpretation of the scarce archaeological finds from the Erzgebirge as remnants from a temporary presence corresponds with the absence of any conclusive evidence for permanent human presence and land-use in palynological records at a regional scale (Seifert-Eulen, 2016). In contrast, human impact on the environment has been observed for underground mining in the Alps during the Bronze Age (Breitenlechner et al., 2013; Schwarz & Oegg, 2013). The oldest geochemical proxy signal that is discussed to derive from possible ore processing in the Erzgebirge is a Pb/As/Cu signal from Kovářská Bog (Cz) with an age estimate of 1540-800 calBC, thus the Middle to Late Bronze Age period (Bohdálková et al., 2018). A drop in the  $^{206}\text{Pb}/^{207}\text{Pb}$  ratio observed at the Bozi Dar peatbog is dated to approx. 2.2 ka calBP (Veron et al., 2014), i.e. corresponding to the Iron Age. Although some studies suggest that tin processing may be detectable by a rising Sn concentration in peats (Meharg et al., 2012) or alluvial sediments (Thorndycraft, Pirrie, & Brown, 2004), no such signal has been observed in layers attributed to Bronze Age mining anywhere so far.

### **The Schellerhau site in the context of Eurasian tin supply**

While Bronze Age tin mining is discussed for the sites of Kestel (Fig. 9.2, (Yener et al., 1989) and Hisarcık (Fig. 9.3,(Yener et al., 2015) in Anatolia, evidence for the exploitation of smaller tin deposits in Eastern Europe like Mount Cer (Serbia) (Fig. 9.5) are rather unassertive (Huska et al., 2014). Recent investigations at mining sites in Tajikistan, Uzbekistan (Garner, 2013), and Iran (Nezafati, Pernicka, & Momenzadeh, 2006), as well as the still contested reading of



Assyrian cuneiforms texts from Karum Kanesh (Klengel, 2009), Mari (Joannes, 1991) and Tell al-Rimah (Reiter, 1997; Faist, 2001), may indicate substantial tin supply of the Near East from eastern sources during the second millennium BC. For Central Europe, tin slags from Brittany (Fig. 9.16, (Mahé-le Carlier, Lulzac, & Giot, 2001) and Cornwall (Fig. 9.14&15, (Penhallurick, 1986; Tylecote, Photos, & Earl, 1989;)) are strong indicators for the local processing of tin ores during the Bronze Age. Further support for early tin placer mining and processing in Cornwall is expected by a reinvestigation and 14C-dating of antler picks that have been discovered during the 19th century in the Carnon Valley near Truro and are very likely related to mining activities (Timberlake 2017). On the Iberian Peninsula the site Cerro de San Cristóbal at Logrosán (Fig. 9.45) provides the oldest archaeological evidence so far for structures related to tin placer processing in the 8th century BC, thus the very end of the Bronze Age (Rodríguez Díaz et al., 2013). Concerning long-distance trade of tin, the ingots recovered from the shipwrecks of Uluburun (Fig. 9.6, (Hauptmann, Maddin, & Prange, 2002), Cape Geledonia (Fig. 9.7, (Bass et al., 1967) and Kefar Samir (Fig. 9.8, (Raban & Galili, 1985) are key evidence for the transport of larger tin quantities in the Mediterranean, while the wreck-site of Salcombe (Fig. 9.9, (Wang et al., 2016) may represent comparable long-distance trade in the Atlantic region. These data are supplemented by inland finds of single ingots reported from Säckinggen (Fig. 9.10), Sursee-Gammainseli (Fig. 9.11), and Zürich-Mozartstraße (Fig. 9.12, all Switzerland, (Nielsen, 2014) and poorly preserved remains from Mochlos (Fig. 9.13, Greece, (Whitley, 2005), and an ingot from the mid-3rd millennium from Alacahöyük (Fig. 9.42, Turkey, (Yalçın, 2016). Recent studies have pointed out that there is a considerable number of personal adornments like beads, rings, pendants, and decorative applications made of tin that may be also related to some kind of raw material circulation (Krüger et al., 2012; Nielsen, 2014).

The indicators for human activities related to tin mining at Schellerhau in the early 2nd millennium coincide on a regional scale with the establishment of the Únětice culture in an area from Central Germany to Bohemia and Moravia in the late 3rd millennium BC and the spread of tin-copper alloys (Krause, 2003). Typological ties of the spearhead in the hoard of Kyhna to the eastern Mediterranean area (Coblenz, 1986) and the existence of rich burials like Leubingen (1942 ± 10 BC dendrochronology) or Helmsdorf (1840 ± 10 BC dendrochronology, Becker et al., 1989) have been discussed to mirror the rise of local elites that were based on the control of long-distance exchange networks (Gerloff, 2010). Later evidence for the establishment of larger political entities around the Erzgebirge area may be provided by the battlefield of the Tollensetal (approx. 1300 calBC), where remains of more

than 130 individuals indicate that larger groups could be deployed and operate over a long distance as some combatants may have originated from Bohemia (Price et al., 2017). In general, the exchange of resources has often been discussed as the decisive formative element in the establishment of regional authorities during the Bronze Age (Kristiansen & Larsson, 2005).. Later activities at Schellerhau during the 15th/14th century BC coincide with the onset of the Lusatian culture in the wider region but any supporting evidence for mining, ore processing and distribution in this area for this cultural context is rather limited (Kytlicová, 2007, pp. 221–224). In summary, the cultural development in the wider region shows a high degree of socio-economic organisation and may have been capable of establishing and supporting tin mining operations beyond the permanent settled core areas as well as introducing the material into the raw-material circulation and exchange networks.

### Conclusions

A major problem is the ephemeral character of the archaeological features that can be expected on extensive placer mining sites, especially as they have usually been reworked during the medieval period. Focussing on locally preserved layers associated with human activities therefore provides a promising approach in this archaeological setting. Our results strongly support the hypothesis that tin placer mining occurred in the upper Erzgebirge outside the prehistorically permanently settled area during the Early Bronze Age period in the early 2nd millennium BC as well as the Middle Bronze Age period. While the cultural development in the wider region does not conflict with the concept of tin placer mine operating in this remote area, any speculations on the intensity and duration of these Bronze Age activities are impossible based on the geoarchaeological record alone.

Resuming tin placer mining from the Medieval period onwards had a strong impact on the existing geoarchaeological record. Although these intensive later activities may mask the Bronze Age record in most European tin districts, the results of our study provide encouragement that investigations in Medieval mining zones may not be futile when it comes to the reconstruction of prehistoric mining activities.

### Acknowledgments

This research was generously funded by the European Union as part of the project Interreg VA “ArchaeoMontan 2018” and the Landesamt für Archäologie Sachsen. Soil analyses were kindly performed by A. Körle (Berlin). We thank the Staatsbetrieb Sachsenforst for the permission of our fieldwork as well as two anonymous reviewers, who helped to improve the manuscript with helpful comments.

## Data Availability Statement

The data that support the findings of this study are available from the corresponding author upon reasonable request.

## Conflict of Interest

The authors declare that they have no conflict of interest.

## *Literature*

AG Boden, A. G. (2005). *Bodenkundliche Kartieranleitung*. Hannover: BGR.

Agricola, G. (1556). *De re metallica libri XII*. Basel: Hieronymus Froben & Nicolaus Episcopus

Annable, F. K., & Simpson, D. D. A. (1964). *Guide catalogue of the Neolithic and Bronze Age collections in Devizes Museums*. Wiltshire: Archaeological & Natural History Society.

Bartelheim, M., & Niederschlag, E. (1998). Untersuchungen zur Buntmetallurgie, insbesondere des Kupfers und Zinns, im sächsisch-böhmischen Erzgebirge und dessen Umland. *Arbeits- und Forschungsberichte zur sächsischen Bodendenkmalpflege*, 40, 8–87.

Bartelheim, M., Niederschlag, E., & Rehren, T. (1998). Research into prehistoric metallurgy in the Bohemian/Saxon Erzgebirge. In B. Hänsel (Ed.), *Mensch und Umwelt in der Bronzezeit Europas: Man and environment in European Bronze Age* (pp. 225–229). Kiel: Oetker-Voges.

Bass, G. F., Throckmorton, P., Taylor, J. D. P., Hennessy, J. B., Shulman, A. R., & Buchholz, H.-G. (1967). Cape Gelidonya: A Bronze Age Shipwreck. *Transactions of the American Philosophical Society*, 57, 1-177.

Becker, B., Jäger, K.-D., Kaufmann, D., & Litt, T. (1989). Dendrochronologische Datierungen von Eichenholzern aus den frühbronzezeitlichen Hügelgräbern bei Helmsdorf und Leubingen (Aunjetitzer Kultur) und an bronzezeitlichen Flußeichen bei Merseburg. *Jahresschrift für mitteldeutsche Vorgeschichte*, 72, 299–312.

Berger, D. (2014). Composition and decoration of the so-called Zinnfigurenstreifen found in Magdeburg, Saxony-Anhalt, Germany. *Restaurierung und Archäologie*, 7, 65–80.

Berglund, B. W., & Ralska-Jasiewiczowa, M. (1986). Pollen analysis and pollen diagrams. In B. E. Berglund (Ed.), *Handbook of Holocene Palaeoecology and Palaeohydrology* (pp. 357–373). Chichester: John Wiley & Sons.

Beug, H.-J. (2004). *Leitfaden der Pollenbestimmung für Mitteleuropa und angrenzende Gebiete*. München: Pfeil.

Bohdálková, L., Bohdál, P., Břízová, E., Pachrová, P., & Kuběna, A. A. (2018). Atmospheric metal pollution records in the Kovářská Bog (Czech Republic) as an indicator of anthropogenic activities over the last three millennia. *Science of the Total Environment*, 633, 857–874.

Bouzek, J., Koutecký, D., & Simon, K. (1989). Tin and prehistoric mining in the Erzgebirge (Ore Mountains): some new evidence. *Oxford Journal of Archaeology*, 8, 203–212.

Breitenlechner, E., Goldenberg, G., Lutz, J., & Oeggel, K. (2013). The impact of prehistoric mining activities on the environment: a multidisciplinary study at the fen Schwarzenbergmoos (Brixlegg, Tyrol, Austria). *Vegetation History and Archaeobotany*, 22, 351–366.

Brügmann, G., Berger, D., Frank, C., Marahrens, J., Nessel, B., & Pernicka, E. (2017). Tin Isotope Fingerprints of Ore Deposits and Ancient Bronze. In P. Newman (Ed.), *The Tinworking Landscape of Dartmoor in a European Context*. Papers presented at a conference in Tavistock Devon 6.-11. May 2016 (pp. 103–114). Dartmoor Tinworking Research Group.

Brügmann, G., Berger, D., Pernicka, E., & Nessel, B. (2015). Zinn-Isotope und die Frage nach der Herkunft prähistorischen Zinns. In T. Gluhak, S. Greiff, K. Kraus, & M. Prange (Eds.), *Archäometrie und Denkmalpflege 2015* (pp. 189–191). Bochum: Deutsches Bergbaumuseum.

Bullock, P. (Ed.). (1985). *Handbook for soil thin section description*. Albrighton: Waine.

Cappers, R. T. J., Bekker, R. M., & Jans, J. E. A. (2012). *Digitale zadenatlas van Nederland = Digital seed atlas of the Netherlands*. Eelde: Barkhuis.

Clark, R. L. (1984). Effects on charcoal of pollen preparation procedures. *Pollen et Spores*, 26, 559–576.

Coblenz, W. (1986). Ein frühbronzezeitlicher Verwahrfund von Kyhna, Kr. Delitzsch. *Arbeits- und Forschungsberichte zur sächsischen Bodendenkmalpflege*, 30, 37–88.

Durcan, J. A., King, G. E., & Duller, G. A. T. (2015). DRAC: Dose rate and age calculator for trapped charge dating. *Quaternary Geochronology*, 28, 54–61.

Emler, J. (1882). *Regesta diplomatica necnon epistolaria Bohemiae et Moraviae II. Annorum 1253-1310*. Prag: Gregerianis.

Faist, B. (2001). Die Handelsbeziehungen zwischen Assyrien und Anatolien in der zweiten Hälfte des 2. Jts. v. Chr. unter besonderer Berücksichtigung des Metallhandels. In H. Klinkott (Ed.), *Anatolien im Lichte kultureller Wechselwirkungen. Akkulturationsphänomene in Kleinasien und seinen Nachbarregionen während des 2. und 1. Jahrtausends v. Chr.* (pp. 53–66). Tübingen: Attempto.

FAO (Ed.). (2006). *World reference base for soil resources, 2006: a framework for international classification, correlation, and communication*. Rome: FAO.

Fedkin, A. V., Seltmann, R., & Förster, H.-J. (2001). Li-bearing micas as a fractionation indicator of tin granites: The Sadisdorf-Schellerhau granite suite, eastern Erzgebirge. In A. Piestrzyński (Ed.), *Mineral deposits at the beginning of the 21st Century: proceedings of the joint sixth Biennial SGA-SEG Meeting, Kraków, Poland, 26-29 August 2001* (pp. 409–412). Lisse: Balkema.

Fox, A. (1957). Excavations on Dean Moor in the Avon Valley 1954-56. *Transactions of the Devonshire Association*, 98, 18–77.

Galbraith, R. F., Roberts, R. G., Laslett, G. M., Yoshida, H., & Olley, J. M. (1999). Optical dating of single and multiple grains of quartz from Jinnium Rock Shelter, northern Australia: Part I, experimental design and statistical models. *Archaeometry*, 41, 339–364.

Garner, J. (2013). *Die montanarchäologischen Forschungen an den Zinnlagerstätten*. Darmstadt: Zabern.

Gerloff, S. (2010). Von Troja an die Saale, von Wessex nach Mykene – Chronologie, Fernverbindungen und Zinnrouten der Frühbronzezeit Mittel- und Westeuropas. In H. Meller & F. Bertemes (Eds.), *Der Griff nach den Sternen. Wie Europas Eliten zu Macht und Reichtum kamen* (pp. 603–639). Halle (Saale): Landesamt f. Denkmalpflege u. Archäologie Sachsen-Anhalt.

Gersbach, E. (1969). *Urgeschichte des Hochrheins*. Bd. 2 Katalog. Freiburg: Kehr.

Glasbergen, W. (1956). De dolk van Bargerooterveld I. *Vonstomstandigheden & beschrijving*. *Nieuwe Drentse Volksalmanak*, 74, 191–198.

Hammermüller, M. (1964). *Um Altenberg, Geising und Lauenstein. Ergebnisse der heimatkundlichen Bestandsaufnahme im Gebiet von Altenberg und Fürstenwalde*. Berlin: Akademie-Verlag.

Hauptmann, A., Maddin, R., & Prange, M. (2002). On the Structure and Composition of Copper and Tin Ingots Excavated from the Shipwreck of Uluburun. *Bulletin of the American Schools of Oriental Research*, 1–30.

Haustein, M., Gillis, C., & Pernicka, E. (2010). Tin isotopy—a new method for solving old questions. *Archaeometry*, 52, 816–832.

Haveman, E., Sheridan, J. A., Shortland, A., & Eremin, K. (2005). The Exloo necklace: new light on an old find. *Palaeohistoria*, 47/48, 101–139.

Hemker, C., & Elburg, R. (2013). ArchaeoMontan - Mittelalterlicher Bergbau in Sachsen und Böhmen. Aufgaben und Ziele des grenzübergreifenden Projektes. In R. Smolnik (Ed.), *ArchaeoMontan 2012: Erkunden - Erfassen - Erforschen. Internationale Fachtagung Dippoldiswalde 18. bis 20. Oktober 2012* (pp. 7–18). Dresden: Landesamt für Archäologie.

Hilmes, M., & Wohl, E. (1995). Changes in channel morphology associated with placer mining. *Physical Geography*, 16, 223–242.

Huska, A., Powell, W., Mitrović, S., Bankoff, H. A., Bulatović, A., Filipović, V., & Boger, R. (2014). Placer Tin Ores from Mt. Cer, West Serbia, and Their Potential Exploitation during the Bronze Age. *Geoarchaeology*, 29, 477–493.

James, A. (1999). Time and the persistence of alluvium: River engineering, fluvial geomorphology, and mining sediment in California. *Geomorphology*, 31, 265–290.

James, L. A. (1991). Incision and morphologic evolution of an alluvial channel recovering from hydraulic mining sediment. *Geological Society of America Bulletin*, 103, 723–736.

Joannes, F. (1991). L'étain, de Elam à Mari. In L. D. Meyer & H. Gasche (Eds.), *Mésopotamie et Elam* (pp. 67–76). Ghent: University of Ghent.

Jones, A. M. (2016). *Preserved in the peat: an extraordinary Bronze Age burial on Whitehorse Hill, Dartmoor, and its wider context*. Oxford Philadelphia: Oxbow Books.

Kleber, A., Terhorst, B., Bullmann, H., Hülle, D., Leopold, M., Müller, S., Raab, T., Sauer, D., Scholten, T., Dietze, M., Felix-Henningsen, P., Heinrich, J., Spies, E.-D., & Thiemeyer, H. (2013). Subdued Mountains of Central Europe. *Developments in Sedimentology*, 66, 9–93.

Klengel, H. (2009). Altassyrischer Zinnhandel mit Anatolien. *TÜBA-AR Türkiye Bilimler Akademisi Arkeoloji Dergisi*, 12, 175–181.

Knighton, A. D. (1987). Tin Mining and Sediment Supply to the Ringarooma River, Tasmania, 1875–1979. *Australian Geographical Studies*, 25, 83–97.

Königer, J. (2005). Unterwasserarchäologie am Überlinger See – Sondagen und Prospektionsarbeiten unter Wasser. *Nachrichtenblatt Arbeitskreis Unterwasserarchäologie*, 11/12, 63–70.

Krause, R. (2003). *Studien zur kupfer- und frühbronzezeitlichen Metallurgie zwischen Karpatenbecken und Ostsee*. Rahden/Westf: Leidorf.

Kristiansen, K., & Larsson, T. B. (2005). *The Rise of Bronze Age Society. Travels, Transmissions and Transformations*. Cambridge: Cambridge University Press.

Krüger, J., Nagel, F., Nagel, S., Jantzen, D., Lampe, R., Dräger, J., Lidke, G., Mecking, O., Schüler, T., & Terberger, T. (2012). Bronze Age tin rings from the Tollense valley in northeastern Germany. *Praehistorische Zeitschrift*, 87, 29–43.

Kytlicová, O. (2007). *Jungbronzezeitliche Hortfunde in Böhmen*. Stuttgart: F. Steiner.

Lehmann, J., & Präger, F. (1992). Reliefentwicklung und periglaziäre Schuttdecken im oberen Erzgebirge. In K. Billwitz, W. Janke, & K.-D. Jäger (Eds.), *Jungquartäre Landschaftsräume* (pp. 110–126). Berlin, Heidelberg: Springer Berlin Heidelberg.

Mahé-le Carlier, C., Lulzac, Y., & Giot, P.-R. (2001). Etude des déchets de réduction provenant de deux sites d'exploitation d'étain armoricain de l'Age du Bronze et du Moyen Age. *Revue archéologique de l'ouest*, 18, 45–56.

Marahrens, J., Berger, D., Brüggemann, G., & Pernicka, E. (2015). Vergleich der stabilen Zinn-Isotopenzusammensetzung von Kassiteriten aus Europäischen Zinn-Lagerstätten. In S. Greiff, A. Kronz, F.

Schlütter, & M. Prange (Eds.), *Archäometrie und Denkmalpflege 2016* (pp. 190–193). Bochum: Deutsches Bergbaumuseum.

Massy, K. (2018). *Die Gräber der Frühbronzezeit im südlichen Bayern. Kallmünz: Lassleben.*

Meharg, A. A., Edwards, K. J., Schofield, J. E., Raab, A., Feldmann, J., Moran, A., Bryant, C. L., Thornton, B., & Dawson, J. J. C. (2012). First comprehensive peat depositional records for tin, lead and copper associated with the antiquity of Europe's largest cassiterite deposits. *Journal of Archaeological Science*, 39, 717–727.

Moore, P. D. ., Webb, J. A., & Collinson, M. E. (1991). *Pollen analysis*. Oxford: Blackwell.

Möslein, S., & Rieder, K. H. (1997). Zinnperlen aus einem frühbronzezeitlichen Grab von Buxheim, Lankreis Eichstätt, Oberbayern. *Archäologisches Jahr in Bayern*, 1997, 68–70.

Muhly, J. D. (1985). Sources of Tin and the Beginnings of Bronze Metallurgy. *American Journal of Archaeology*, 89, 275–291.

Müller, A., Seltmann, R., & Behr, H.-J. (2000). Application of cathodoluminescence to magmatic quartz in a tin granite - case study from the Schellerhau Granite Complex, Eastern Erzgebirge, Germany. *Mineralium Deposita*, 35, 169–189.

Murray, A., & Wintle, A. (2000). Luminescence dating of quartz using an improved single-aliquot regenerative dose protocol. *Radiation Measurements*, 32, 57–73.

Nelson, A. D., & Church, M. (2012). Placer mining along the Fraser River, British Columbia: The geomorphic impact. *Geological Society of America Bulletin*, 124, 1212–1228.

Nessel, B., Brüggmann, G., & Pernicka, E. (2015). Tin isotopes and the sources of tin in the Early Bronze Age Unetice culture. In J. M. Mata-Perelló, M. A. Hunt Ortiz, & E. Orche Garcia (Eds.), *Patrimonio geológico y minero: de la investigación a la difusión* (pp. 1–19). Logrosán.

Nezafati, N., Pernicka, E., & Momenzadeh, M. (2006). Ancient tin: Old question and a new answer. *Antiquity*, 80, 3–6.

Niederschlag, E., Pernicka, E., Seifert, T., & Bartelheim, M. (2003). The Determination of Lead Isotope Ratios by Multiple Collector ICP-MS: A Case Study of Early Bronze Age Artefacts and their Possible Relation With Ore Deposits of the Erzgebirge. *Archaeometry*, 45, 61–100.

Nielsen, E. H. (2014). A Late Bronze Age tin ingot from Sursee-Gammainseli (Kt. Luzern). *Archäologisches Korrespondenzblatt*, 44, 177–193.

Oberdorfer, E. (2001). *Pflanzensoziologische Exkursionsflora für Deutschland und angrenzende Gebiete*. Stuttgart: Ulmer.

Penhallurick, R. D. (1986). *Tin in antiquity: its mining and trade throughout the ancient world with particular reference to Cornwall*. Leeds: Maney for the Institute of Materials, Minerals and Mining.

Price, T. D., Frei, R., Brinker, U., Lidke, G., Terberger, T., Frei, K. M., & Jantzen, D. (2017). Multi-isotope proveniencing of human remains from a Bronze Age battlefield in the Tollense Valley in northeast Germany. *Archaeological and Anthropological Sciences* [in press].

Primas, M. (1984). Bronzezeitlicher Schmuck aus Zinn. *Helvetica Archaeologica*, 15, 33–42.

Pulak, C. (2009). The Uluburun tin ingots and the shipment of tin by sea in the Late Bronze Age Mediterranean. *Turkish Academy of Sciences Journal of Archaeology*, 12, 188–207.

Raban, A., & Galili, E. (1985). Recent maritime archaeological research in Israel-A preliminary report. *International Journal of Nautical Archaeology*, 14, 321–356.

Rahmstorf, L. (2016). The use of bronze objects in the third millennium BC – a survey between Atlantic and Indus. In J. Maran & P. Stockhammer (Eds.), *Appropriating innovations. Entangled knowledge in Eurasia, 5000–1500 BCE* (pp. 184–210). Oxford: Oxbow.

- Randsborg, K., & Christensen, K. (2006). *Bronze Age oak-coffin graves*. Archaeology & dendro-dating. Kopenhagen: Blackwell Munksgaard.
- Reimer, P. (2013). IntCal13 and Marine13 Radiocarbon Age Calibration Curves 0–50,000 Years cal BP. *Radiocarbon*, 55, 1869–1887.
- Reiter, K. (1997). *Die Metalle im Alten Orient unter besonderer Berücksichtigung altbabylonischer Quellen*. Münster: Ugarit-Verlag.
- Roden, C. (1985). Montanarchäologische Quellen des ur- und frühgeschichtlichen Zinnerzbergbaus in Europa. *Der Anschnitt*, 37, 50–80.
- Rodríguez Díaz, A., Pavón Soldevila, I., Duque Espino, D. M., Ponce de León Iglesias, M., Hunt Ortiz, M. A., & Merideth, C. (2013). La explotación tartésica de la casiterita entre los ríos Tajo y Guadiana: San Cristóbal de Logrosán (Cáceres). *Trabajos de Prehistoria*, 70, 95–113.
- Schwarz, A. S., & Oeggl, K. (2013). Vegetation change during the Bronze Age studied in a multi-proxy approach: Use of wood linked to charcoal analysis. *Vegetation History and Archaeobotany*, 22, 493–507.
- Schwarzenberg, H., Massy, K., & Mahnke, S. (2014). Ein frühbronzezeitlicher Knochenknebel mit Zinnstiften aus Poing, Lkr. Ebersberg. *Bayerische Vorgeschichtsblätter*, 79, 23–29.
- Schweingruber, F. H. (1990). *Anatomie europäischer Hölzer*. Bern: Haupt.
- Seifert-Eulen, M. (2016). Die Moore des Erzgebirges und seiner Nordabdachung. *Vegetationsgeschichte ausgewählter Moore*. *Geoprofil*, 14, 4–78.
- Stebich, M. (1995). *Beiträge zur Vegetationsgeschichte des Georgenfelder Hochmoores*. Dissertation Universität Leipzig. Leipzig.
- Stöllner, T., Breitenlechner, E., Fritsch, D., Gontscharov, A., Hanke, K., Kirchner, D., Kovács, K., Moser, M., Nicolussi, K., Oeggl, K., Pichler, T., Pils, R., Prange, M., Thiemeyer, H., & Thomas, P. (2010). Ein Nassaufbereitungskasten vom Troiboden. Interdisziplinäre Erforschung des bronzezeitlichen Montanwesens am Mitterberg (Land Salzburg, Österreich). *Jahrbuch des Römisch-Germanischen Zentralmuseums*, 57, 1–32.
- Stoops, G. (2003). *Guidelines for analysis and description of soil and regolith thin sections*. Madison: Soil Science Soc. of America.
- Thorndycraft, V. R., Pirrie, D., & Brown, A. G. (2004). Alluvial records of medieval and prehistoric tin mining on Dartmoor, southwest England. *Geoarchaeology*, 19, 219–236.
- Timberlake, S. (2017). New ideas on the exploitation of copper, tin, gold, and lead ores in Bronze Age Britain: The mining, smelting, and movement of metal. *Materials and Manufacturing Processes*, 32, 709–727.
- Tylecote, R. F., Photos, E., & Earl, B. (1989). The composition of tin slags from the south-west of England. *World Archaeology*, 20, 434–445.
- Veron, A., Novak, M., Břízová, E., & Stepanova, M. (2014). Environmental imprints of climate changes and anthropogenic activities in the Ore Mountains of Bohemia (Central Europe) since 13 cal. kyr BP. *The Holocene*, 24, 919–931.
- Wagenbreth, O. (Ed.). (1990). *Bergbau im Erzgebirge: technische Denkmale und Geschichte*. Leipzig: Dt. Verl. für Grundstoffindustrie.
- Wang, Q., Strekopytov, S., Roberts, B. W., & Wilkin, N. (2016). Tin ingots from a probable Bronze Age shipwreck off the coast of Salcombe, Devon: Composition and microstructure. *Journal of Archaeological Science*, 67, 80–92.
- Whitley, J. (2005). Archaeology in Greece 2004–2005. *Archaeological Reports*, 51, 1–118.
- Wintle, A. G., & Murray, A. S. (2006). A review of quartz optically stimulated luminescence characteristics and their relevance in single-aliquot regeneration dating protocols. *Radiation Measurements*, 41, 369–391.

Yalçın, Ü. (2016). Zinn für die Königin. Ein Barrenfragment aus Alacahöyük und seine Deutung. In G. Körlin, M. Prange, T. Stöllner, & Ü. Yalçın (Eds.), *From bright ores to shiny metals. Festschrift for Andreas Hauptmann on the occasion of 40 years research in Archaeometallurgy and Archaeometry* (pp. 69–74). Bochum: Marie Leidorf.

Yener, K. A., Kulakoğlu, F., Yazgan, E., Kontani, R., Hayakawa, Y. S., Lehner, J. W., Dardeniz, G., Öztürk, G., Johnson, M., Kaptan, E., & Hacı, A. (2015). New tin mines and production sites near Kültepe in Turkey: a third-millennium BC highland production model. *Antiquity*, 89, 596–612.

Yener, K. A., Özbal, H., Kaptan, E., Pehlidotvan, A. N., & Goodway, M. (1989). Kestel: An Early Bronze Age Source of Tin Ore in the Taurus Mountains, Turkey. *Science*, 244, 200–203.



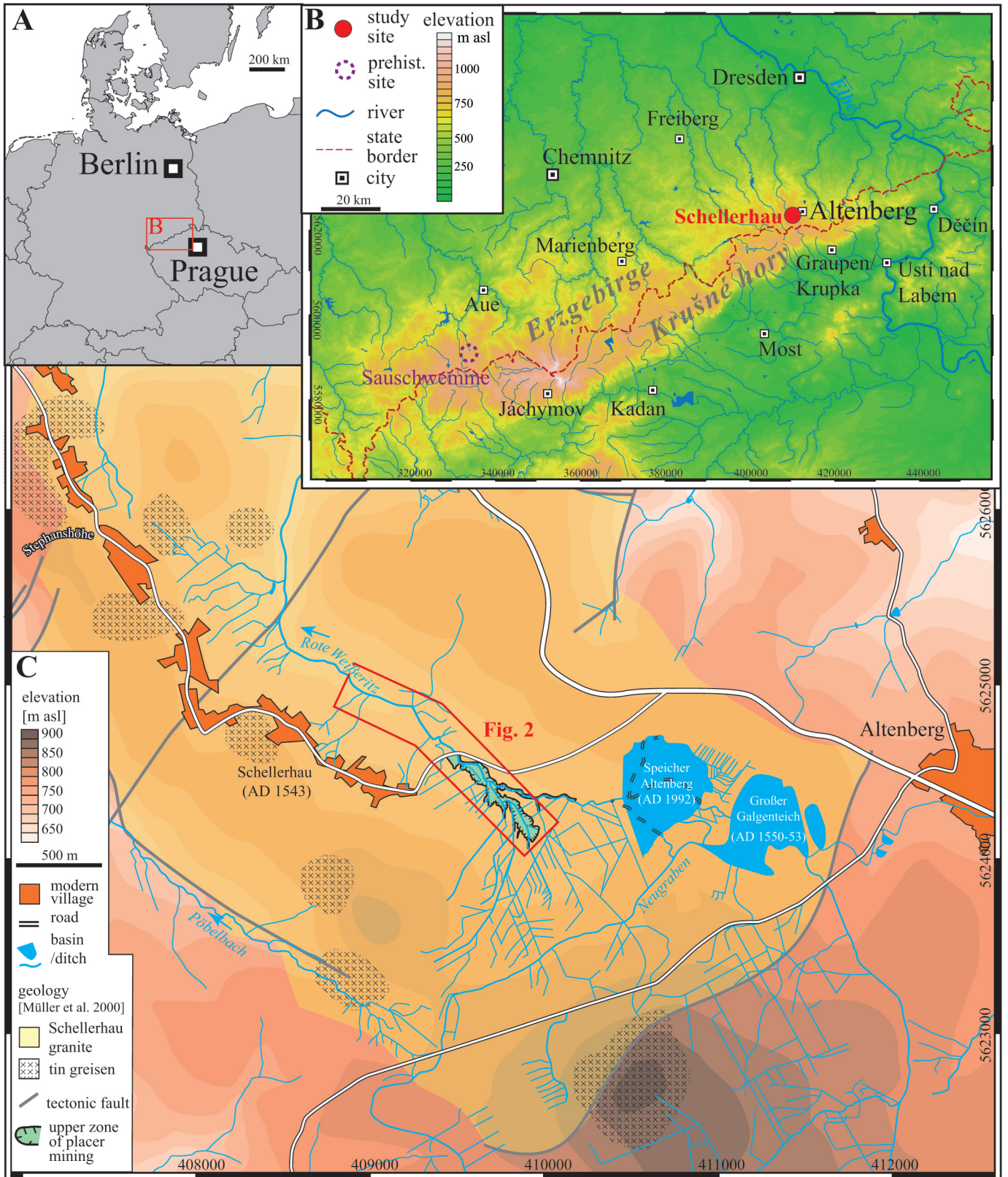


Fig. 1: A: Location of the Schellerhau site; B: The Schellerhau site in the Erzgebirge / Krušné hory area; C: Geology and Topography

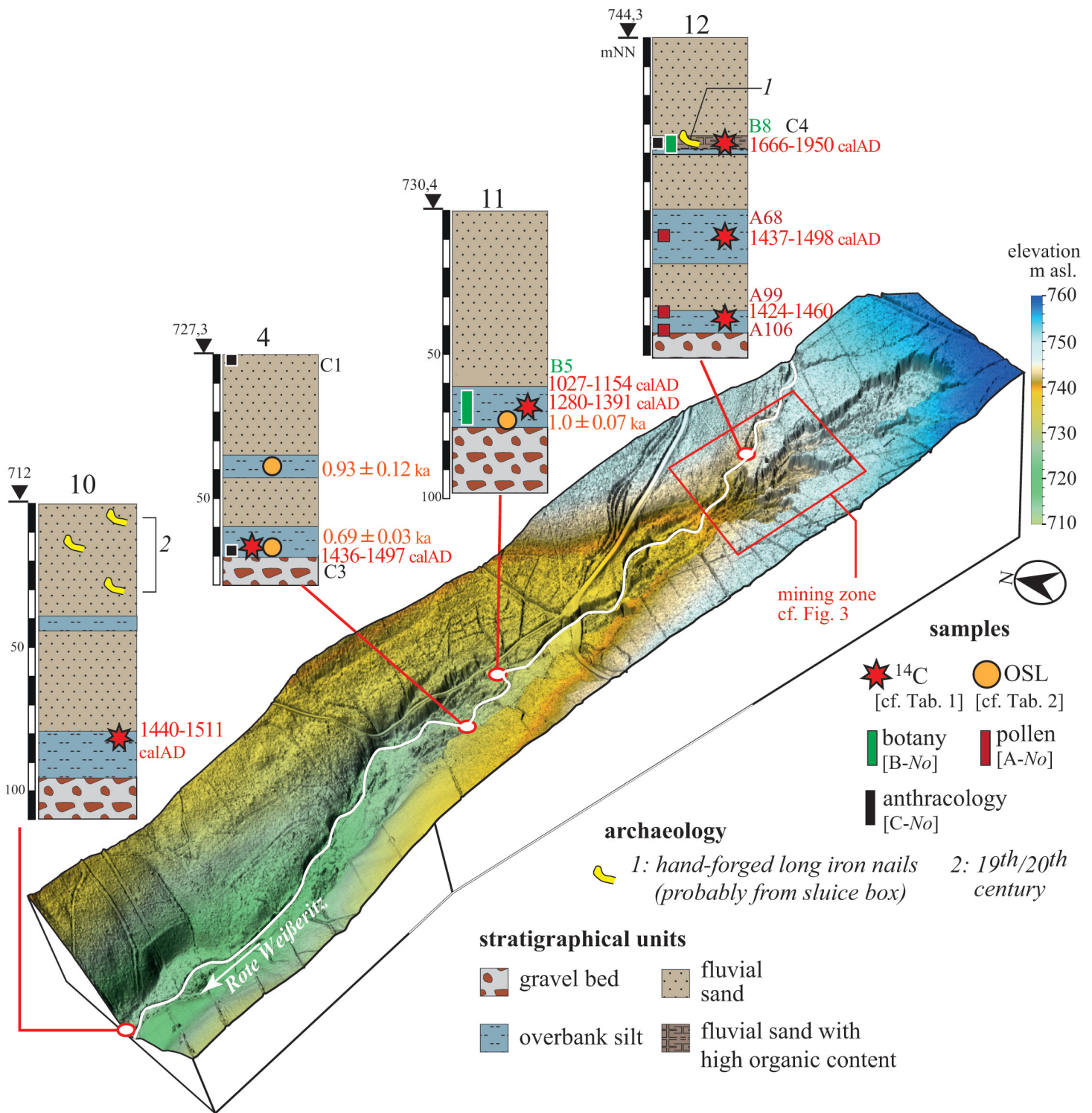


Fig. 2: Digital elevation model (DEM) of the site with simplified stratigraphic logs and sampling positions from the downstream sedimentation zone.



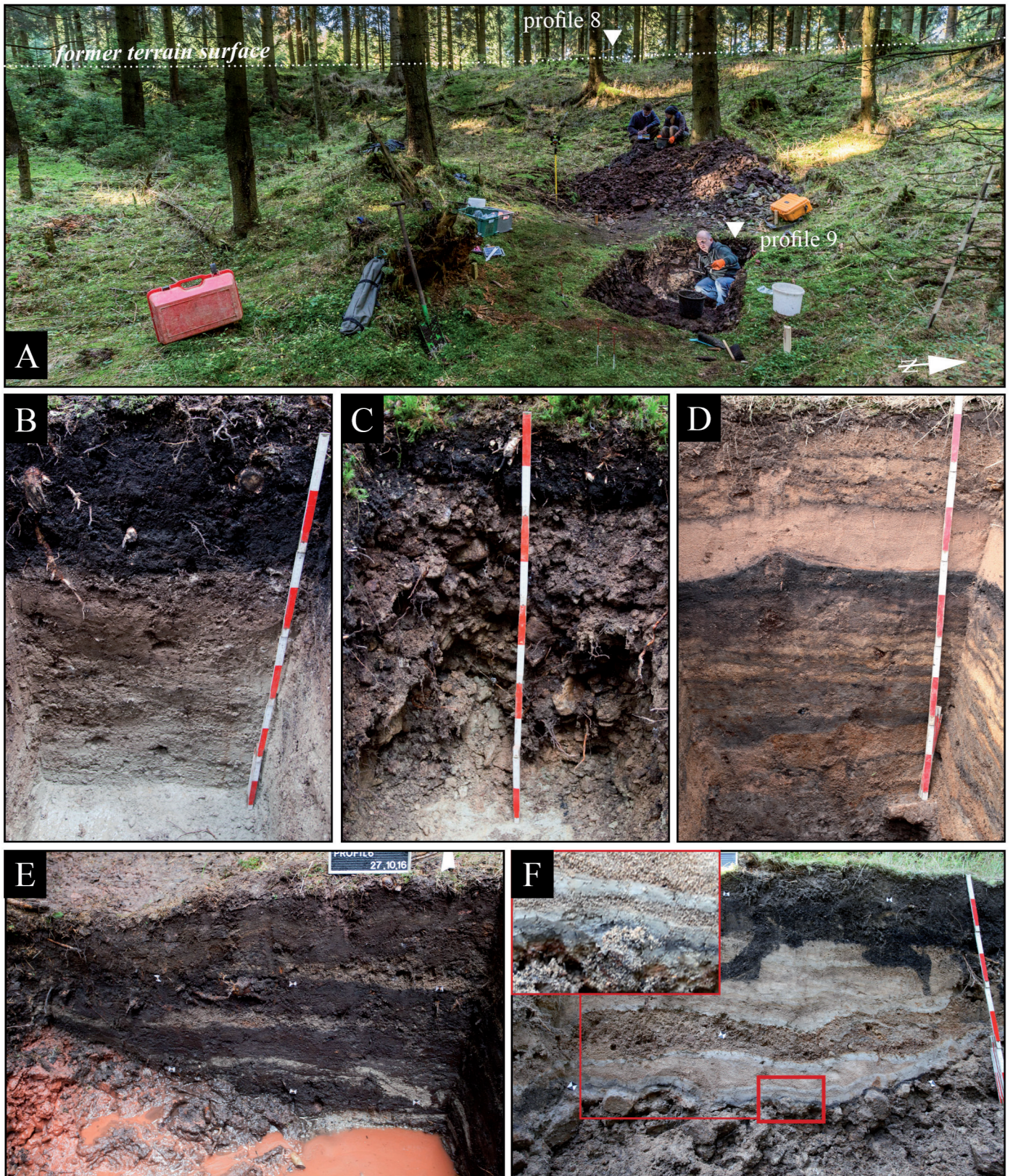


Fig. 3: Selected topographic situations and stratigraphies; A: Situation of profile 9 in an area where soil material has been removed artificially (photo: M. Jehnichen); B: reference profile 8 outside the mining area, scale units= 10cm; C: piled-up gravels from placer mining in profile 5; D: Fluvial fines and fluvial sands in profile 12; E: Profile 6 in an abandoned ditch structure filled with peat and fluvial sands; F: Fluvial fines and fluvial sands in profile 4, detail inset: thinly layered fluvial fines and charcoal layer.



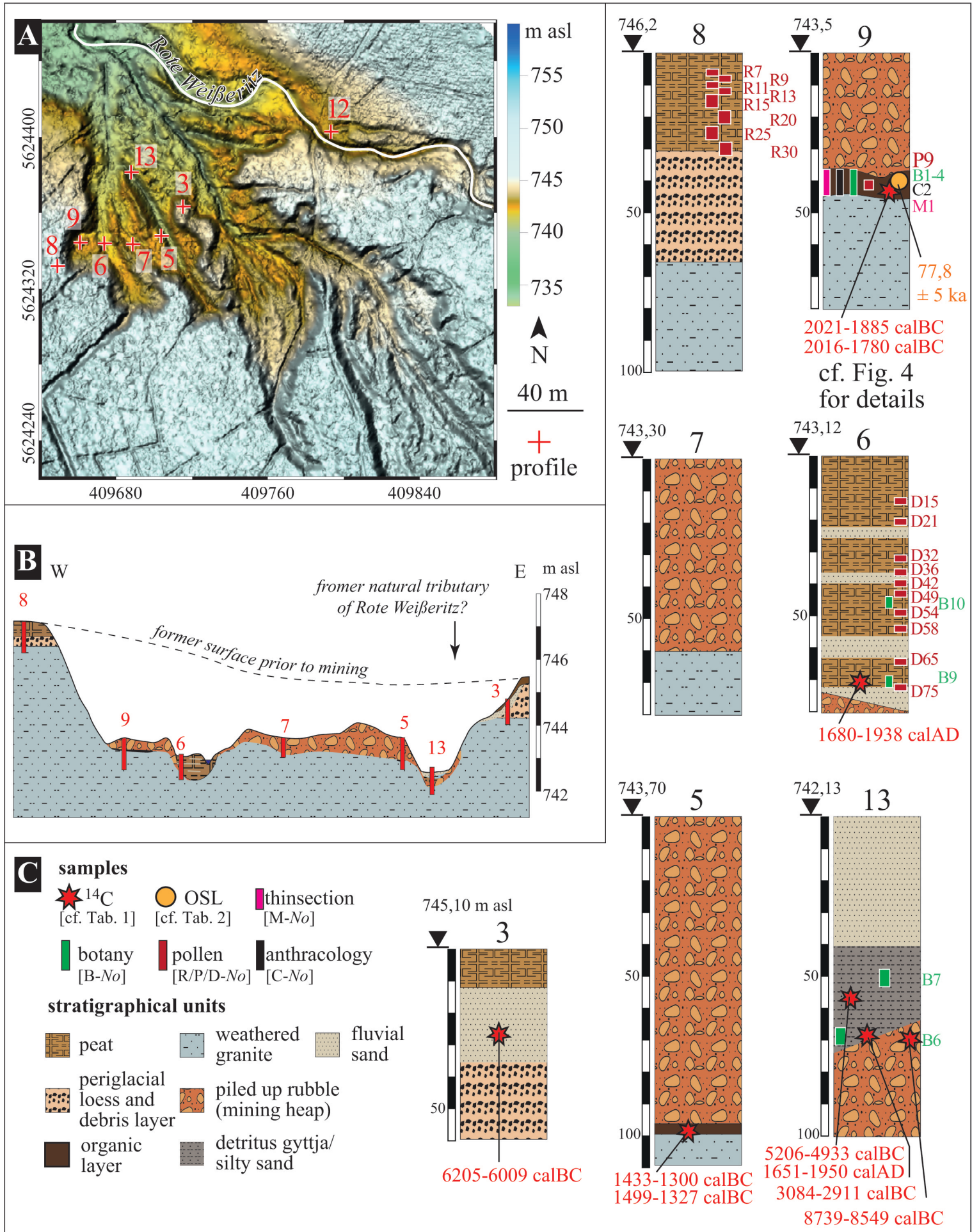


Fig. 4: A: DEM from the mining zone with the location of the profiles; B: Idealised W-E cross-section through the extraction zone, C: simplified stratigraphic logs of profiles and sampling positions



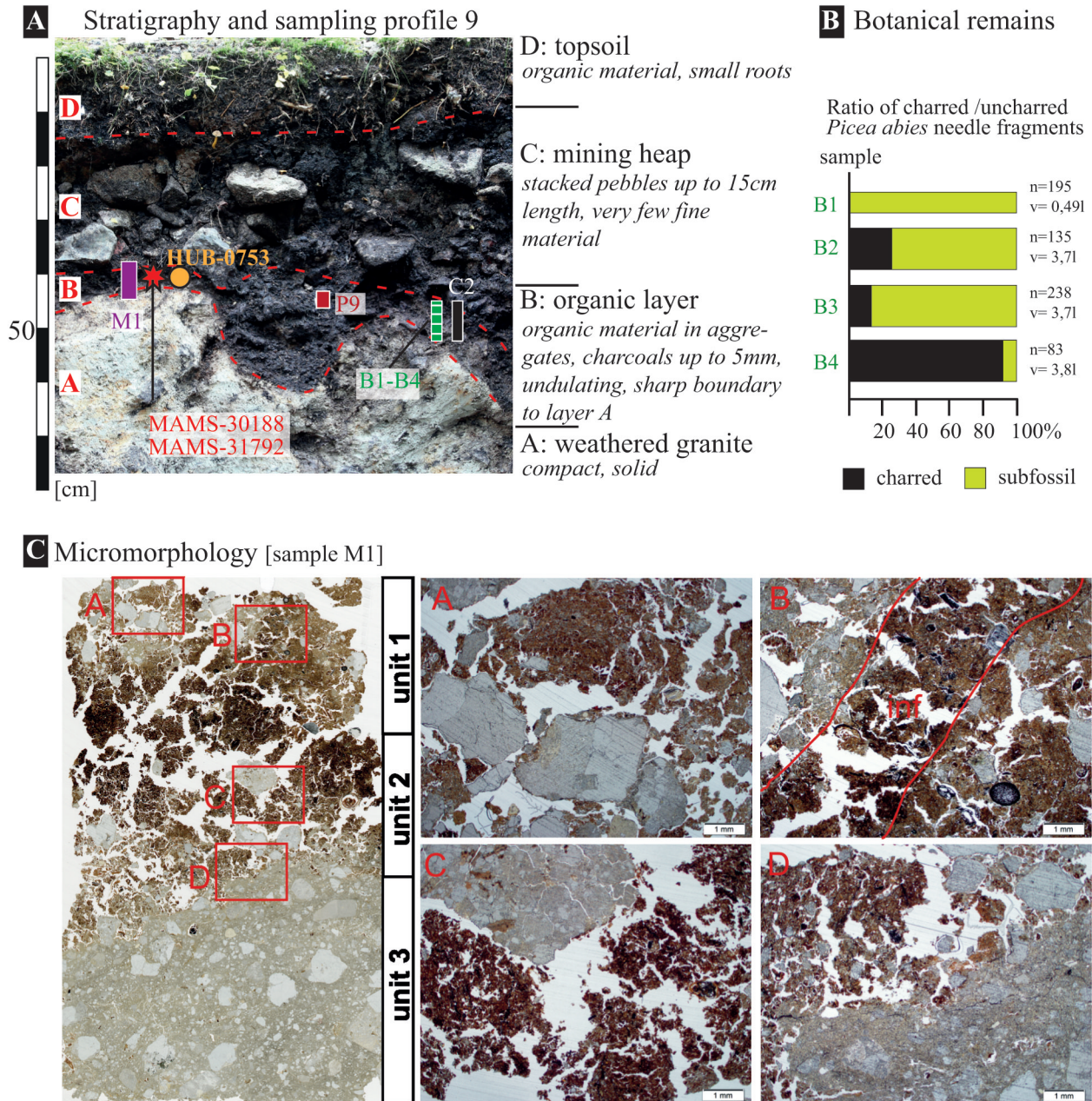


Fig. 5: A: Photo of the stratigraphic situation in profile 9 with zonation; 4B: Ratio of charred/uncharred *Picea abies* needles within the organic layer on top of the granite. 4C: Scan of the thin section (width: 4.5 cm) M1; Microphotos (A-D, plain polarized light): A: unit 1, subangular blocky microstructure and granite fragments, B: unit 1, more densely packed with dense incomplete infilling (inf) with material from unit 2 - richer in organic matter and charcoal, C: unit 2, material highly affected by bioturbation, D: sharp boundary between unit 2 and unit 3.

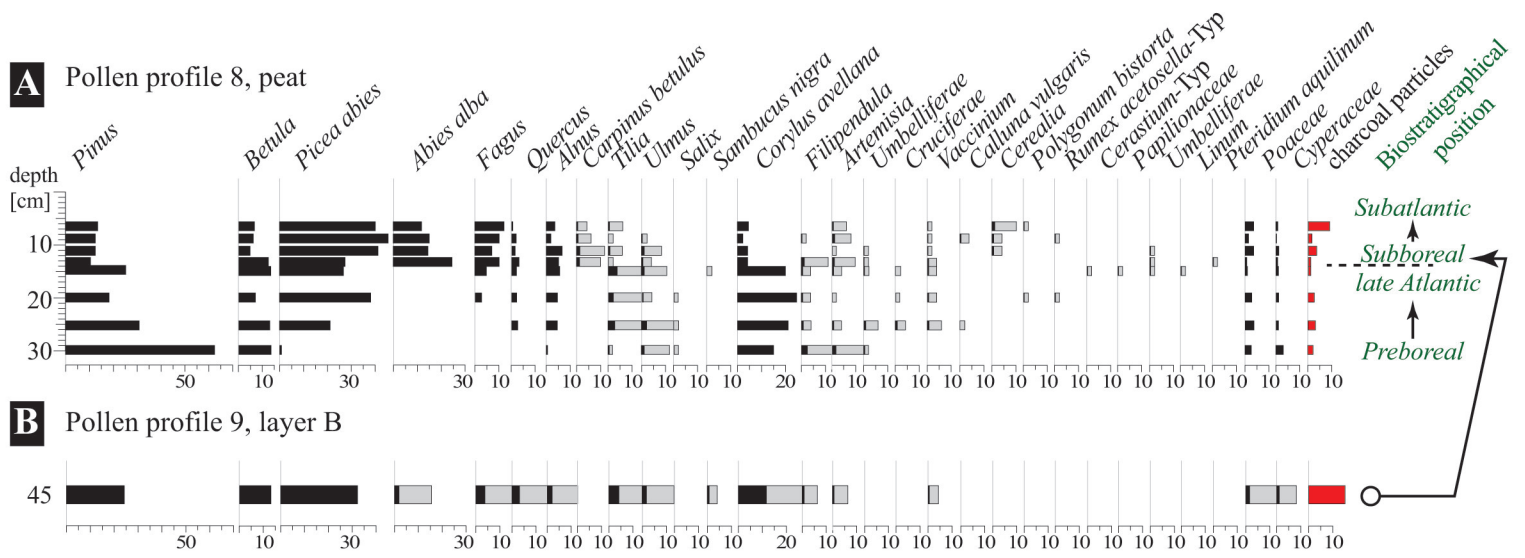


Fig. 6: A: Palynological results from profile 8 outside the mining area, B: Palynological spectrum from profile 9, layer B

**mining zone**

profile 3 MAMS-28839

profile 6 MAMS-30240

profile 13

MAMS-34615

MAMS-32529  
MAMS-32528  
stratigraphically inverted

MAMS-33868

profile 9 MAMS-31792  
MAMS-30188

profile 5 MAMS-33873  
MAMS-31407

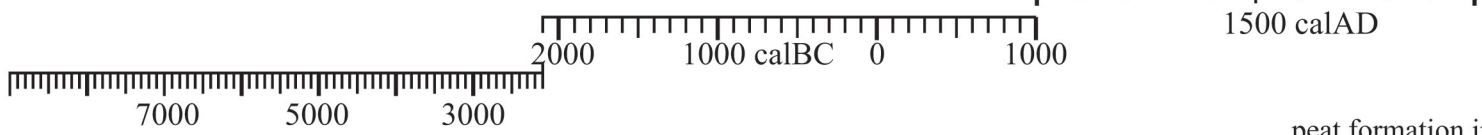
**alluvial records**

profile 12 MAMS-31793  
MAMS-31791  
MAMS-32964

profile 11 MAMS-33865  
MAMS-31409  
HUB-0754

profile 4 HUB-0752  
HUB-0751  
MAMS-28840

profile 10 MAMS-32963



**site formation**

peat formation in abandoned ditches



**regional archaeological / historical context**

Mesolithic

Neolithic

Bronze Age

Únětice C.

Lusatian C.



[key sites, see text]

Nebra sky disk

Tollensetal battlefield

1305AD historical evidence for tin mining at Graupen

1446AD acquisition of area by Friedrich II

1436/40AD tin mining at Altenberg

Fig. 7: Chronological results from the mining area and downstream sedimentation zone and inferred phases of site formation together with regional archaeological zonation and historical data



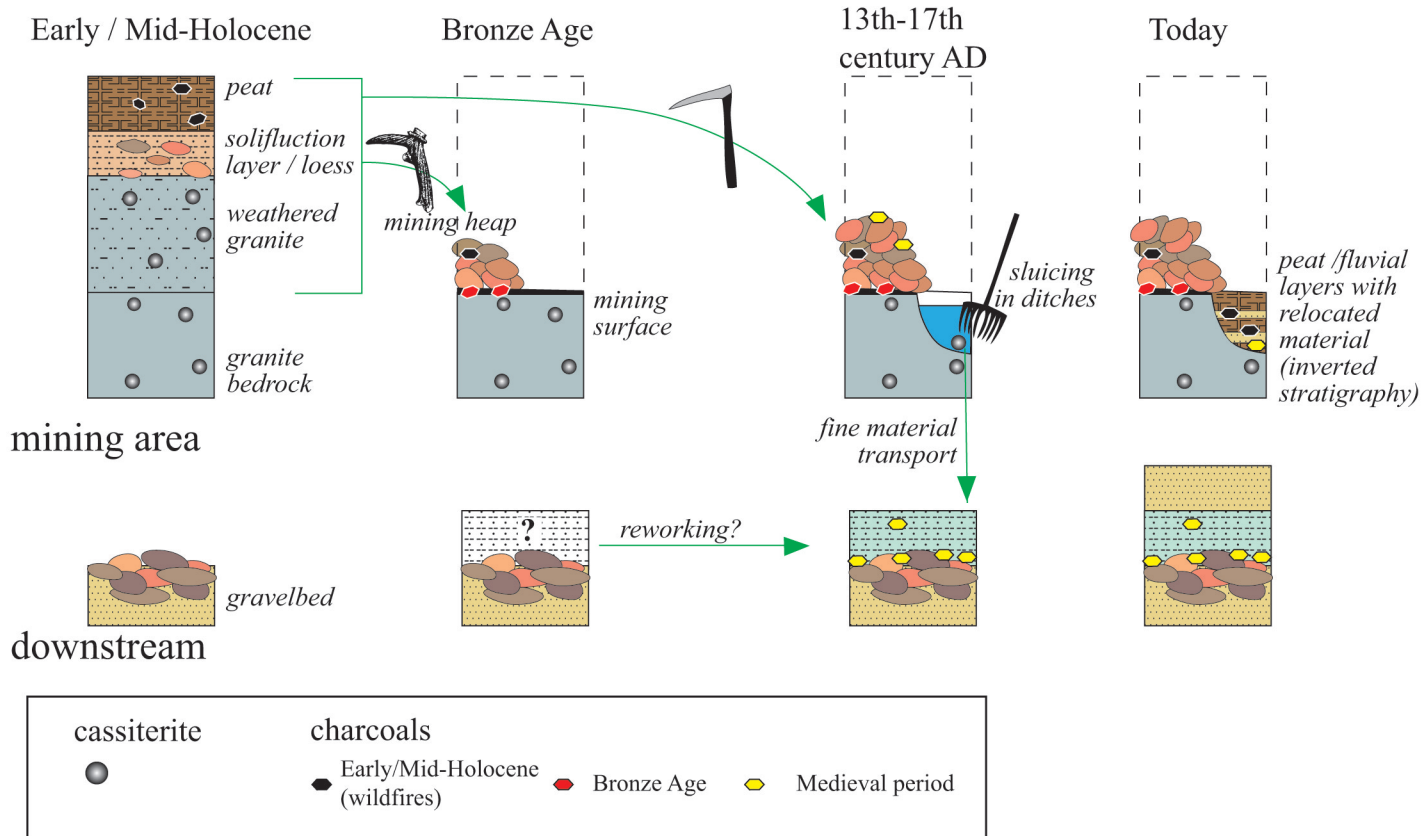


Fig. 8: Idealised development of stratigraphic units in the mining area and the downstream zone.



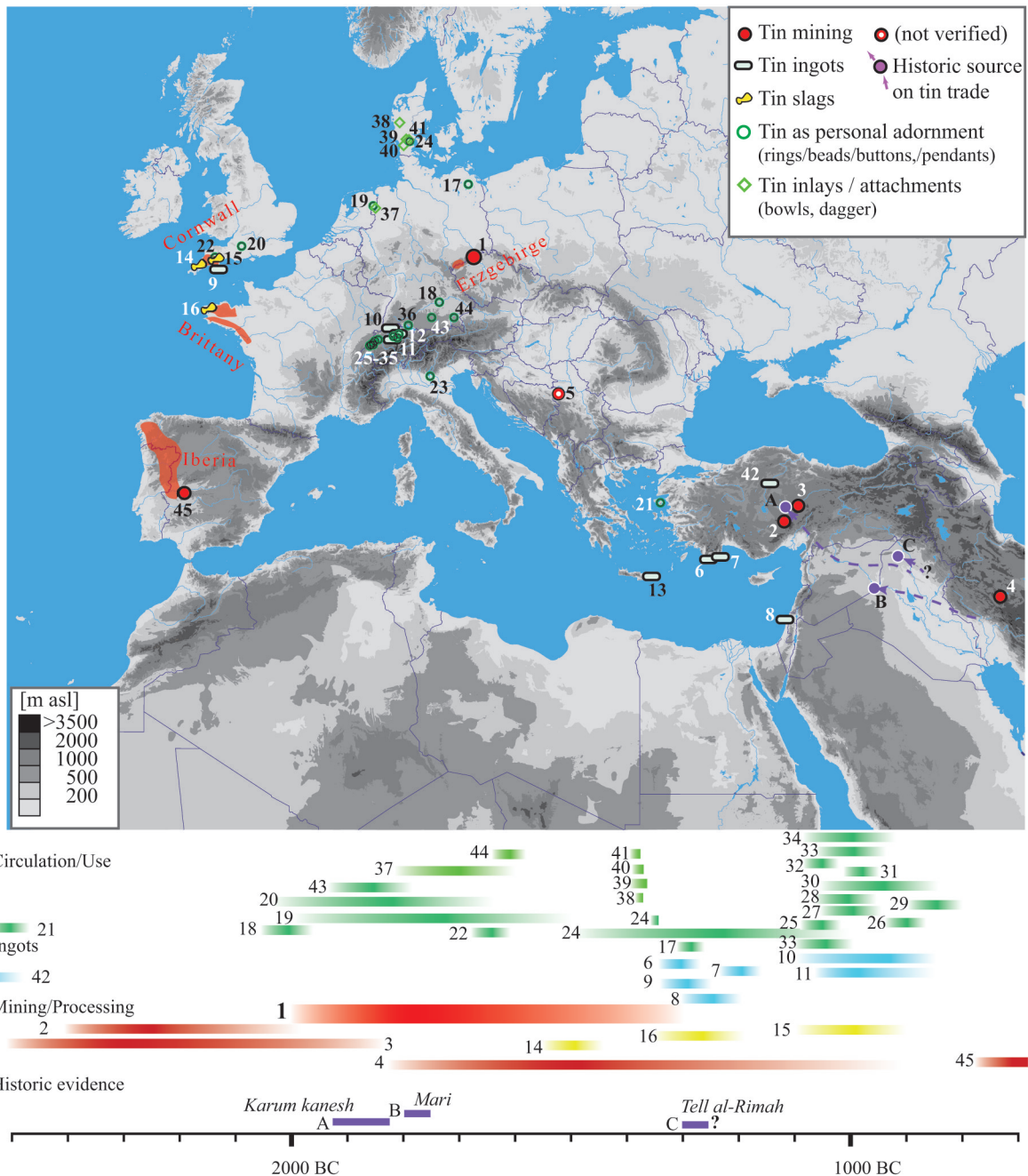


Fig. 9: Map of Bronze Age sites related to tin mining or processing as well as tin ingots and objects possibly indicating exchange networks and tin circulation routes. 1: Schellerhau (this study); 2: Kestel (Yener et al., 1989); 3: Hisarcik (Yener et al., 2015); 4: Deh Hosein (Nezafati, Pernicka, & Momenzadeh, 2006); 5: Mount Cer (Huska et al., 2014); 6: Uluburun shipwreck (Hauptmann, Maddin, & Prange, 2002; Pulak, 2009); 7: Cape Gelydonia shipwreck (Bass et al., 1967); 8: Kefar Samir shipwreck (Raban & Galili, 1985); 9: Salcombe shipwreck (Wang et al., 2016); 10: Säcking (Gersbach, 1969); 11: Sursee-Gammainseli; 12: Zürich-Mozartstraße (Nielsen, 2014); 13: Mochlos (Whitley, 2005); 14: Caerloggas (Penhallurick, 1986; Tylecote, Photos, & Earl, 1989); 15: Dean Moor (Fox, 1957); 16: St. Renan (Mahé-le Carlier, Lulzac, & Giot, 2001); 17: Tollensetal (Krüger et al., 2012); 18: Buxheim (Möslein & Rieder, 1997); 19: Exloo (Haveman et al., 2005); 20: Sutton Veny (Annable & Simpson, 1964); 21: Thermi (Muhly, 1985); 22: Whitehorse Hill (Jones, 2016); 23: Peschiera (Primas, 1984); 24: Trindhøj grave C (Randsborg & Christensen, 2006); 25: Hitzkirch-Moos; 26: Zug-Sumpf; 27: Zürich-Wollishofen; 28: Zürich- Großer Haffner; 29: Möringen; 30: Hauterive-Champréveyres; 31: Cortaillod-Est; 32: Concise (Vaud); 33: Grandson-Corcelettes; 34: Onnens; 35: Estavayer-le-Lac; (Nielsen, 2014); 36: Unteruhldingen-Stollenwiesen (Königer, 2005); 37: Bargerosterveld (Glasbergen, 1956); 38: Storehøj Barde; 39: Store Kongehøj; 40: Lille Dragshøj; 41: Guldhøj A outer grave (Randsborg & Christensen, 2006); 42: Alacahöyük grave A (Yalçın, 2016); 43: Schwabmünchen-Mittelstetten, 44: Poing (Schwarzenberg, Massy, & Mahnke, 2014; Massy, 2018); 45: Cerro de San Cristóbal (Rodríguez Díaz et al., 2013)

LabNo.	profile, depth below surface, context	material	<sup>14</sup> C	<sup>14</sup> C (calibrated; IntCal13, 1σ)	<sup>14</sup> C (calibrated ; IntCal13, 2σ)	δ <sup>13</sup> C (AM S)
			[BP]	[calBC/ calAD]	[calBC/ calAD]	[‰]
MAMS-28839	profile 3, 30 cm depth, fluvial sands	charcoal particle indet.	7210 ± 30	6082-6024	6205-6190 6184-6140 6114-6009	-23,5
MAMS-28840	profile 4, 73 cm depth, charcoal layer in basal overbank silt	charcoal particle indet.	409 ± 21	1445-1473	1436-1497 1600-1615	-20,6
MAMS-30188	profile 9, 55- 60 cm depth, layer with charcoal	charcoal ( <i>Picea abies</i> )	3586 ± 25	1963-1896	2021-1992 1984-1885	-22,4
MAMS-30240	profile 6, 70-75 cm depth, basal peat layer in ditch	uncharred needles ( <i>Picea abies</i> )	126 ± 20	1684-1706 1720-1734 1806-1819 1832-1880 1915-1929	1680-1764 1801-1894 1906-1938	-39,1
MAMS-31407	profile 5, 100 cm below mining heap	charcoal particle indet.	3110 ± 23	1420-1384 1340-1311	1433-1371 1359-1300	-28,9
MAMS-31409	profile 11, 68 cm depth, charcoal layer in basal overbank silt	charcoal particle indet.	942 ± 21	1033-1050 1084-1125 1136-1150	1027-1154	-23,2
MAMS-31791	profile 12, 68 cm depth, charcoal from middle overbank silt	charcoal particle indet.	408 ± 22	1444-1475	1437-1498 1508-1510 1600-1616	-25,3
MAMS-31792	profile 9, 55- 60 cm depth, layer with charcoal	charcoal ( <i>Picea abies</i> )	3567 ± 26	1946-1886	2016-1996 1980-1876 1842-1819 1976-1780	-27,4
MAMS-31793	profile 12, 40 cm depth, layer with charcoals and iron nails	charcoal ( <i>Picea abies</i> )	157 ± 23	1670-1690 1729-1778 1798-1810 1926-1943	1666-1699 1721-1784 1795-1818 1832-1880 1916-	-25,7
MAMS-32528	profile 13, 75cm depth, organic gyttja in ditch	charcoal particle indet.	4370 ± 25	3011-2978 2972-2925	3084-3066 3028-2911	-23,2
MAMS-32529	profile 13, 62 cm depth,	charcoal particle indet.	6069 ± 28	5052-4977 4971-4964	5206-5166 5116-5111	-26,2

	organic silt in ditch				5078-4933	
MAMS-32963	profile 10, 90 cm depth	charcoal, ( <i>Abies alba</i> )	401 ± 20	1446-1480	1440-1511 1600-1616	-21,8
MAMS-32964	profile 12, 102 cm depth, charcoal from lowermost overbank silt	charcoal particle indet.	448 ± 19	1434-1450	1424-1460	-15,0
MAMS-33865	profile 11, 68 cm depth, charred organic in basal overbank silt	charred particles ( <i>Rubus idaeus</i> , <i>Sambucus niger</i> , <i>Picea abies</i> )	657 ± 23	1287-1305 1364-1385	1280-1319 1351-1391	-23,1
MAMS-33868	profile 13, 62 cm depth, organic silt in ditch	uncharred needles ( <i>Picea abies</i> )	201 ± 22	1661-1678 1765-1800 1940-	1651-1684 1736-1805 1935-	-30,6
MAMS-33873	profile 5, 100 cm below mining heap	charcoal particles indet.	3156 ± 26	1490-1484 1452-1410	1499-1393 1333-1327	-26,8
MAMS-34615	profile 13, 62 cm depth, in mining heap	charcoal particles indet.	9359 ± 35	8701-8676 8647-8571	8739-8549	-24,5

Table 1: <sup>14</sup>C results

LabNo.	profile, depth below surface [cm], elevation [m asl], H <sub>2</sub> O content [% weight]	D <sub>E</sub> measurement parameters	<sup>238</sup> U	<sup>232</sup> Th	<sup>40</sup> K	D <sub>0</sub> Dose rate	D <sub>E</sub> Equivalent dose	OSL ages
			[ppm]	[ppm]	[ppm]	[Gy/ka]	[Gy]	[ka] / [AD]
	*1	*2	*3	*3	*3		*4	*5
HUB-0751	profile 4, 73 cm depth,, charcoal layer in basal overbank silt, 727 m asl, 30 ± 5 % H <sub>2</sub> O	preheat: 240°C; 2mm stencil recycling ratio: 0,9-1,1 recuperation < 10% OSL IR depletion ratio >0,9	9,68 ± 0,39	42,12 ± 1,94	3,58 ± 0,06	6,6 ± 0,23	4,53± 0,15 (CAM)	<b>0,69 ± 0,03 ka</b> <b>1326 ± 30 AD</b>
HUB-0752	profile 4, 40 cm depth, 25 ± 5 % H <sub>2</sub> O	preheat: 200°C; 2mm stencil recycling ratio: 0,9-1,1 recuperation < 10% OSL IR depletion ratio >0,9	6,97 ± 0,29	31,91 ± 1,48	3,85 ± 0,06	6,1 ± 0,22	5,65± 0,73 (MAM2)	<b>0,93 ± 0,12 ka</b> <b>1086 ± 120 AD</b>
HUB-0753	profile 9, 55-60 cm depth, layer with charcoal, 40 ± 10 % H <sub>2</sub> O	preheat: 200°C; 1mm stencil recycling ratio: 0,9-1,1 recuperation < 10% OSL IR depletion ratio >0,9	15,22 ± 0,84 ( <sup>226</sup> Ra) /	2,81 ± 0,23	2,81 ± 0,23	6,24 ± 0,39	485,89 (MEAN)	<b>77,83 ± 5,12 ka</b>
			29,3 ± 1,9 ( <sup>238</sup> U)			8,42 ± 0,54		57,68 ± 3,88 ka
HUB-0754	profile 11, 65 cm, 25 ± 5 % H <sub>2</sub> O	preheat: 200°C; 2mm stencil recycling ratio: 0,9-1,1 recuperation < 10% OSL IR depletion ratio >0,9	10,61 ± 0,59	3,7 ± 0,37	3,7 ± 0,37	7,11 ± 0,36	8,36± 0,78 (MAM1)	1,23 ± 0,13 ka
							6,77± 0,32 (LOW)	<b>1,0 ± 0,07 ka</b> <b>1016 ± 70 AD</b>

\*1 grain size fraction used: 90-200 µm

\*2 Tl/OSL-DA-15C7C unit, <sup>90</sup>Sr/<sup>90</sup>Y radiation emitter with 0,085 Gy/s

\*3 measured by gamma ray spectroscopy (HUB-0751/-752 at Cologne University; HUB-0753/-754 at VKTA Dresden)

\*4 CAM= Central Age Model; MAM1= Minimum Age Model with overdispersion σ b=0,1; MAM2= Minimum Age Model with overdispersion σ b=0,2; MEAN= mean with standard deviation; LOW = based on lowest aliquot

\*5 Ages displayed in Fig. 6 are bold

Sample [B= macro-remains; C= anthracology] cf. Fig. 2/3 for sample location				B1	B2	B3	B4	B5	B6	B7	B8	B9	B10	C1	C2	C3	C4
Sample size [litre]/[pieces]				0,49l	3,7l	3,7l	3,8l	0,76l	0,3l	0,5l	0,6l	0,3l	0,3l	50pc	50pc	6pc	13pc
Depth [cm] / excavation layer				layer 1	layer 2	layer 3	layer 3	60-68	70-75	55-65	35-40	75	50	10	55	75	45-40
Profile				9	9	9	9	11	13	13	12	6	6	4	9	4	12
	taxonomy	anatomy	preservation														
Forest community	<i>Picea abies</i>	FS	u	2		2											
		ND	ch		34	31	76	29		1		1					
		ND	u	195	101	207	7		47	3000+	280	40+	71				
		C	ch				1										
		C	u	1		2											
		W	ch											35	50	6	13
	<i>Abies alba</i>	W	ch											6			
		ND	u										21				
		R	u									1					
	<i>Oxalis acetosella</i>	FS	u			1						1					
<i>Scirpus sylvaticus</i>	R	u									1						
Forest edges / clearances	<i>Rubus idaeus</i>	FS	ch					3									
		FS	u		2			4					2				
	<i>Sambucus nigra</i>	FS	ch					2									
		FS	u					2									
	<i>Vaccinium myrtillus</i>	FS	u									1					
No specific communities + wetland	<i>Viola spec.</i>	R	u									1					
	<i>Juncus spec.</i>	FS	u	5	144	100	25	50		2							
	<i>Carex spec.</i>	FS	u							2							
	Moss	R	ch		2		6	1									
		R	u	+	+	+	+	+									
	charred [indet.]	R	ch	+	+++	+++	+++	+++	+++	+	+	+++	+	+	9	0	0
Anatomy: FS=fruit/seed, ND=needle, C= cone, W= wood, R= other remains (e.g. bark) Preservation: ch=charred, u=uncharred; Quantity: + = present (>10), ++ = numerous (>100), +++ = abundant (>500)																	

Table 3: Botanical and anthracological results

Unit	Aggregation/pedality	Voids	Microstructure	Material composition/ ratio inorganic : organic	Inclusions roots/charcoal/s clerotia	Post-depositional alterations
1	left part: moderately to strong developed pedality  right part: weakly developed pedality	left: compound packing voids  right: vughs (frequent), cracks (few), channels (few)	left: subangular blocky  right: vughy	80 : 20 inorganic: fragments of granite and its mineral grains; organic: fine material, root residues, roots, sclerotia;  exception: dense incomplete infilling with material of unit 2	roots (frequent), charcoal (few), sclerotia (few)	moderate bioturbation: infillings, roots, channels
2	strongly developed pedality	compound packing voids, cracks (few)	complex: mixture of granular, crumb and subangular blocky	50 : 50 to 40 : 60 inorganic: fragments of granite and its mineral grains; organic: fine material – partly masking mineral grains, roots, root residues, sclerotia, residues of mycorrhiza mantles	roots (frequent), charcoal (frequent), sclerotia (frequent)	strong bioturbation: partly crumb microstructure, roots, loosening of structure, faecal pellets
3	apedal material	cracks (few)	massive	nearly 100% granite; very few roots	roots (very few)	weathering: few cracks and roots

Supporting Information 1: Micromorphological description of sample M1 (profile 9)

Profile ID	Sample ID	Sampling depth	Sediment facies	Soil horizon	Soil horizon	Colour	Grain-size composition, main fractions			Textural class	Grain-size composition, single fractions					Loss-on-ignition		
							Clay <0.002 mm (%)	Silt <0.063 mm (%)	Sand >2 mm (%)		Clay <0.002 mm (%)	Fine silt <0.063 mm (%)	Medium silt <0.02 (%)	Coarse silt <0.063 mm (%)	Fine sand <0.2 (%)		Medium sand <0.63 (%)	Coarse sand <2 mm (%)
		(cm)		(KA5) <sup>1</sup>	(FAO) <sup>2</sup>					(KA5)								
3	-	0-15	Peat	Ha	Ha	greyish brown	-	-	-	-	-	-	-	-	-	-	-	
3	KG-88	15-35	Fluvial (sand)	II Go	2CI	grey	1,7	13,9	84,4	Su2	1,7	5,5	5,1	3,3	5,2	38,4	40,8	2,1
3	-	35-50	Fluvial (gravel to cobble)	III Go	3CI	grey-brown	-	-	-	-	-	-	-	-	-	-	-	-
4	-	0-20	Fluvial (sand)	Ah	Ah	black	-	-	-	-	-	-	-	-	-	-	-	-
4	-	20-38	Fluvial (sand)	Go	CI	yellow-grey	-	-	-	-	-	-	-	-	-	-	-	-
4	KG-96	38-42	Fluvial (silt)	II Go	2CI	grey	5,5	66,2	28,3	Us	5,5	27,9	27,3	11,0	25,6	2,7	0,0	2,0
4	KG-95	42-47	Fluvial (sand)	III Go	3CI	yellow-grey	3,8	32,2	64,1	Su3	3,8	14,3	13,5	4,4	7,4	39,0	17,7	1,1
4	KG-94	47-49	Fluvial (silt)	IV Go	4CI	grey	7,7	73,4	18,9	Us	7,7	23,0	28,7	20,7	15,6	3,3	0,0	2,5
4	KG-93	49-60	Fluvial (sand)	V Go	5CI	yellow-grey	-	-	-	-	-	-	-	-	-	-	-	1,2
4	KG-92	60-62	Fluvial (silt)	VI Go	6CI	grey	7,0	78,5	14,5	Us	7,0	22,0	29,3	27,2	12,9	1,6	0,0	2,1
4	KG-91	62-66	Fluvial (sand)	VII Go	7CI	yellow-grey	1,8	16,1	82,1	Su2	1,8	8,5	7,0	0,6	1,1	38,1	42,9	0,9
4	KG-90	66-70	Fluvial (silt)	VIII Gr	8Cr	grey	6,4	76,3	17,3	Us	6,4	25,2	29,0	22,1	15,7	1,5	0,1	2,6
4	KG-89	70-73	Fluvial (silt with charcoal)	VIII Gr	8Cr	black	6,5	76,9	16,6	Us	6,5	17,3	26,4	33,2	12,8	3,5	0,3	7,6
5	-	0-18	Mining rubble (sand)	yAh	Ahu	black	-	-	-	-	-	-	-	-	-	-	-	-
5	-	18-28	Mining rubble (gravel)	II yGo	2Clu	brown	-	-	-	-	-	-	-	-	-	-	-	-
5	-	28-60	Mining rubble (gravel and stones)	III yGo	3Clu	brown	-	-	-	-	-	-	-	-	-	-	-	-
5	-	60-100	Mining rubble (gravel and stones with charcoal)	yGo	Clu	grey-brown	-	-	-	-	-	-	-	-	-	-	-	-
5	-	100-110	Weathered granite (silty sand)	II Gr	2Cr	grey	-	-	-	-	-	-	-	-	-	-	-	-
6	KG-97	0-22	Peat	Hv	He	brown	-	-	-	-	-	-	-	-	-	-	-	69,7
6	KG-98	22-30	Fluvial (sand)	II Gr	2Cr	yellow-grey	1,9	24,1	74,1	Su2	1,9	7,6	8,2	8,2	6,6	14,9	52,6	4,5
6	KG-99	30-44	Peat	III fHr	3Heb	brown	-	-	-	-	-	-	-	-	-	-	-	44,3
6	KG-100	44-46	Fluvial (sand)	IV Gr	4Cr	yellow-grey	-	-	-	-	-	-	-	-	-	-	-	3,5
6	KG-101	46-60	Peat	V fHr	5Heb	brown	-	-	-	-	-	-	-	-	-	-	-	66,3
6	KG-102	60-70	Fluvial (sand)	VI Gr	6Cr	yellow-grey	1,6	15,2	83,2	Su2	1,6	4,8	4,8	5,6	8,6	21,6	53,0	2,1
6	KG-103	70-75	Peat	VII fHr	7Heb	brown	-	-	-	-	-	-	-	-	-	-	-	62,4
6	KG-104	75-85	Fluvial (sand)	VIII Gr	8Cr	yellow-grey	-	-	-	-	-	-	-	-	-	-	-	1,5
7	-	0-10	Mining rubble (sand)	yAh	Ahu	black	-	-	-	-	-	-	-	-	-	-	-	-
7	-	10-35	Mining rubble (gravel)	II yGo	2Clu	brown	-	-	-	-	-	-	-	-	-	-	-	-
7	-	35-60	Mining rubble (gravel and stones)	III yGo	3Clu	brown	-	-	-	-	-	-	-	-	-	-	-	-
7	-	60-80	Weathered granite (silty sand)	IV Gr	4Cr	grey-brown	-	-	-	-	-	-	-	-	-	-	-	-
8	KG-105	5-30	Peat	Ha	Ha	black	-	-	-	-	-	-	-	-	-	-	-	92,0
8	KG-106	30-35	Solifluction layer	II rGo-Bh	2BhCI	yellow	4,7	44,5	50,8	Su4	4,7	13,9	16,4	14,2	8,7	16,7	25,4	4,8
8	KG-107	35-57	Loess	III rGo-Bh	3BhCI	yellow-brown	7,4	79,0	13,6	Us	7,4	26,0	31,9	21,1	8,7	4,5	0,4	7,9
8	KG-108	57-75	Weathered granite (gravelly silt)	IV Go	4CI	yellow-grey	6,3	62,0	31,7	Us	6,3	26,5	24,5	11,0	6,2	15,9	9,6	2,0
8	KG-109	75-100	Weathered granite (gravelly silt)	V Gr	5Cr	grey	8,2	76,8	15,0	U12	8,2	33,6	31,1	12,1	5,0	8,6	1,4	1,6
9	-	0-20	Mining rubble (sand)	yAh	Ahu	black	-	-	-	-	-	-	-	-	-	-	-	-
9	-	20-55	Mining rubble (gravel and stones)	II yGo	2Clu	brown	-	-	-	-	-	-	-	-	-	-	-	-
9	M1	55-60	Palaeosol (formed from weathered granite; with charcoal)	III fAh	3Ahb	black	-	-	-	-	-	-	-	-	-	-	-	-
9	-	60-90	Weathered granite (gravelly loamy sand)	Go	3CI	grey	-	-	-	-	-	-	-	-	-	-	-	-
10	KG-113	0-30	Fluvial (sand)	Ah, Go	Ah, CI	black, yellow	2,0	18,5	79,5	Su2	2,0	8,8	8,1	1,6	4,2	51,2	24,1	1,0
10	KG-112	43-48	Fluvial (sand)	II Go	2CI	brown-grey	3,4	43,0	53,6	Su4	3,4	12,7	15,0	15,3	15,2	24,4	14,0	8,0
10	KG-111	80-85	Fluvial (silt)	III Gr	3Cr	brown-grey	4,0	53,6	42,5	Us	4,0	14,7	18,7	20,2	18,9	14,6	9,0	8,0
10	KG-110	85-90	Fluvial (silt)	IV Gr	4Cr	grey	5,1	58,5	36,4	Us	5,1	15,9	18,6	24,0	26,7	8,9	0,8	1,5
11	-	0-30	Fluvial (sand)	Go-Ah, Go	Ah, CI	black, yellow	-	-	-	-	-	-	-	-	-	-	-	-
11	KG-115	30-35	Fluvial (silt)	II Go	2CI	brown	4,2	57,5	38,3	Us	4,2	15,2	19,2	23,1	19,6	13,2	5,5	9,0
11	KG-114	60-68	Fluvial (silt)	III Go	3CI	grey	6,6	79,1	14,3	Us	6,6	31,5	33,1	14,5	10,0	4,3	0,0	2,2
12	KG-116	0-38	Fluvial (sand)	Go-Ah, Go	Ah, CI	black, yellow	2,4	19,2	78,4	Su2	2,4	9,5	8,1	1,6	6,7	58,5	13,2	1,1
12	KG-117	38-45	Palaeosol (formed from fluvial sand)	II fAa	2Ahb	dark brown	3,6	49,5	47,0	Su4	3,6	11,1	15,2	23,2	17,0	19,6	10,4	14,0
12	KG-118	45-60	Fluvial (sand)	III Go	3CI	yellow	2,0	17,8	80,2	Su2	2,0	7,3	7,7	2,8	4,6	49,5	26,1	1,3
12	KG-119	60-75	Fluvial (silt)	IV Go	4CI	grey	6,7	72,8	20,5	Us	6,7	23,4	29,4	20,0	10,4	9,3	0,8	9,1
12	-	75-95	Fluvial (sand)	V Go	5CI	yellow	-	-	-	-	-	-	-	-	-	-	-	-
12	KG-120	95-110	Fluvial (silt)	VI Gr	6Cr	grey	5,1	65,7	29,2	Us	5,1	19,0	25,4	21,3	10,5	12,8	5,9	3,7
13	-	0-20	Fluvial (sand)	Go-Ah	Ah	black	-	-	-	-	-	-	-	-	-	-	-	-
13	-	20-40	Fluvial (sand)	Go	CI	grey-brown	-	-	-	-	-	-	-	-	-	-	-	-
13	-	40-55	Fluvial (sand)	Gr	Cr	yellow	-	-	-	-	-	-	-	-	-	-	-	-
13	KG-135	55-65	Lacustrine (gyttja)	II fF1	2Lrb1	dark grey	4,2	54,6	41,2	Us	4,2	9,3	15,4	29,9	27,0	12,2	2,0	18,4
13	KG-134	65-70	Lacustrine (gyttja)	II fF2	2Lrb2	light grey	5,2	63,0	31,8	Us	5,2	9,4	15,5	38,1	21,3	6,4	4,1	6,1
13	KG-133	70-75	Lacustrine (gyttja)	II fF3	2Lrb3	brown	3,3	40,3	56,4	Su4	3,3	9,3	12,4	18,6	21,4	21,1	13,9	32,7
13	-	75-80	Mining rubble (gravel and stones)	III yGr	3CrU	-	-	-	-	-	-	-	-	-	-	-	-	-

<sup>1</sup>Ad hoc-AG Boden, 2005. Bodenkundliche Kartieranleitung (KA5), 5th edition. Schweizerbart, Hannover.

<sup>2</sup>FAO, 2006. Guidelines for Soil Description, 4th edition. FAO, Rome.